*Human Molecular Genetics, 2008, Vol. 17, No. 19* ***3055–3074***
*doi:10.1093/hmg/ddn203*
*Advance Access published on July 15, 2008*

# TDRD3, a novel Tudor domain-containing protein, localizes to cytoplasmic stress granules

**Isabelle Goulet[1], Sophie Boisvenue[1], Sophie Mokas[2], Rachid Mazroui[2] and Jocelyn Côté[1,*]**

[1]Department of Cellular and Molecular Medicine and Centre for Neuromuscular Disease, Faculty of Medicine, University of Ottawa, Ottawa, ON, Canada K1H 8M5 and [2]Unité de recherche en génétique humaine et moléculaire, Centre de recherche de l'Hôpital Saint-François d'Assise, Université Laval, Québec, QC, Canada G1L 3L5

Received May 21, 2008; Revised and Accepted July 11, 2008

**Our previous work has demonstrated that the Tudor domain of the 'survival of motor neuron' protein and the Tudor domain-containing protein 3 (TDRD3) are highly similar and that they both have the ability to interact with arginine-methylated polypeptides. TDRD3 has been identified among genes whose overexpression has a strong predictive value for poor prognosis of estrogen receptor-negative breast cancers, although its precise function remains unknown. TDRD3 is a modular protein, and in addition to its Tudor domain, it harbors a putative nucleic acid recognition motif and a ubiquitin-associated domain. We report here that TDRD3 localizes predominantly to the cytoplasm, where it co-sediments with the fragile X mental retardation protein on actively translating polyribosomes. We also demonstrate that TDRD3 accumulates into stress granules (SGs) in response to various cellular stresses. Strikingly, the Tudor domain of TDRD3 was found to be both required and sufficient for its recruitment to SGs, and the methyl-binding surface in the Tudor domain is important for this process. Pull down experiments identified five novel TDRD3 interacting partners, most of which are potentially methylated RNA-binding proteins. Our findings revealed that two of these proteins, SERPINE1 mRNA-binding protein 1 and DEAD/H box-3 (a gene often deleted in Sertoli-cell-only syndrome), are also novel constituents of cytoplasmic SGs. Taken together, we report the first characterization of TDRD3 and its functional interaction with at least two proteins implicated in human genetic diseases and present evidence supporting a role for arginine methylation in the regulation of SG dynamics.**

## INTRODUCTION

Cell signaling pathways rely heavily on modular proteins containing protein–protein interaction domains to sense, transmit and process signals that regulate cellular functions (1). The domains involved in these interactions recognize specific peptide motifs in their binding partner, and this recognition can be further influenced by the presence of post-translational modifications, such as phosphorylation, ubiquitination or methylation. These modifications can be either added or removed to create dynamic changes in protein binding properties, thus enabling rapid cellular responses to both external and internal stimuli.

Arginine methylation is a common post-translational modification that has been shown to play central roles in signal transduction pathways regulating many cellular processes, including cell growth, transcription and DNA repair (2–4). Although a number of proteomic screens have now significantly expanded the repertoire of arginine-methylated proteins (5–7), RNA-binding proteins remain a predominant class of the proteins harboring this modification. Consistent with this observation, several studies have also suggested roles for arginine methylation in the regulation of various post-transcriptional processes, including pre-mRNA splicing (8,9), mRNA export (10) and translation (11,12). However, the precise molecular mechanisms involved in the regulation of these processes remain largely unknown. Several lines of evidence support the idea that arginine methylation may serve as an important regulatory signal in these cellular pathways. First, methylated arginines have been shown to be

*To whom correspondence should be addressed. Tel: +1 6135625800 ext. 8660; Fax: +1 6135625636; Email: jcote@uottawa.ca

mainly involved in the regulation of protein–protein interactions (8,13–15). Second, these modified arginines are specifically recognized by a protein module termed 'Tudor domain' (16,17). Third, the recent discovery of enzymes that can remove the methylation mark (18–20) confirms that this modification is dynamic.

The Tudor domain is a 60-amino acid motif that was first discovered through a protein sequence comparison analysis, performed to identify conserved patterns in *Drosophila* Tudor (21,22), a protein involved in germ cell formation that harbors 11 repeated Tudor domains. Tudor domains are highly conserved throughout evolution: they can be found in virtually all organisms, from bacteria to mammals. In the latter, approximately 15 'Tudor Domain-containing proteins' (TDRD1, 2, etc.) can be found in sequence databases; the functions of most remaining largely unknown. The Tudor domain of the 'survival of motor neuron' (SMN) protein, the causative gene for spinal muscular atrophy, is by far the best characterized. Three-dimensional structure determination of the SMN Tudor fold revealed a barrel-like structure composed of β-sheets forming a hydrophobic pocket, surrounded by negatively charged and aromatic residues, which together likely constitute the protein–protein interaction surface (23,24). This structural fold shares similarities with the Chromo domain, a motif known to interact with methylated lysines in histones (25). This resemblance led to the proposition that methyl-substrate binding might be a general feature of these related domains. Several studies have now indeed demonstrated methyl-dependent interactions between the Tudor domain of SMN and a number of arginine-methylated proteins (9,17,26–29). Other studies have also suggested the existence of another subclass of Tudor domains, dubbed 'tandem Tudor', which recognize methylated lysines instead of arginines (16,30). These include the Tudor domains of 53BP1 (31,32) and JMJD2A (33). Taken together, these findings support the notion that the Tudor domain is a *bona fide* 'protein module'.

Interestingly, several of the first Tudor domain-containing proteins that were identified also possessed RNA-binding capacity, which led to the suggestion that Tudor domains may play a role in RNA metabolism (22). Further evidence supporting this hypothesis has now been provided, as common themes are starting to emerge. First, structural analysis of the N-terminal domain of fragile X mental retardation protein (FMRP), a well-characterized KH-containing RNA-binding protein, revealed the presence of a Tudor domain (34). This Tudor-KH configuration is also found in at least one other protein (35). This suggests that these modular proteins could serve as scaffolding proteins involved in the integration of arginine methylation signals and RNA processing. Second, the Tudor-SN protein was shown to participate in both RNA interference and RNA editing pathways (36). Third, SMN promotes the transfer of core Sm proteins to snRNAs in the cytoplasmic assembly of spliceosomal small nuclear ribonucleoprotein particles (snRNPs) (17,37–39), and it is thought to serve as a 'master assembler' of many additional RNP complexes (40–42). Finally, SMN (8,37,43) and two other Tudor domain-containing proteins, SPF30 (44,45) and p100 (46,47), have all been shown to play a role in pre-mRNA splicing. These observations suggest that Tudor domains may serve as molecular adaptors in post-transcriptional processes regulated by arginine methylation.

The TDRD3 is a novel modular protein of unknown function. It was identified among genes whose overexpression has a strong predictive value for poor prognosis of estrogen receptor-negative breast cancers (48). This suggests that TDRD3 may contribute to the progression of breast cancer. Its Tudor domain is highly similar to that of SMN and we have recently demonstrated that it also has the ability to bind arginine-methylated polypeptides (17). In addition to its Tudor domain, TDRD3 harbors a DUF/OB-fold motif (putative nucleic acid recognition motif), as well as a UBA (ubiquitin-binding domain A) domain (49). As suggested by the presence of both nucleic acid- and methyl-binding properties, we speculated that TDRD3 could be central in RNA processing regulatory pathways involving arginine methylation.

In order to gain insight into its cellular function, we generated antibodies against TDRD3 and undertook its biochemical characterization. Immunofluorescence (IF) microscopy studies showed that TDRD3 localizes diffusely in both the cytoplasm and the nucleus. Interestingly, we observed that TDRD3 colocalizes with TIA-1, G3BP and FMRP in cytoplasmic stress granules (SGs) in response to various cellular stresses. SGs become visible at the microscopic level upon various environmental stresses, but recent studies suggest they may represent natural sites of cytoplasmic mRNA sorting/triage that play a major role in the post-transcriptional regulation of gene expression by regulating the localization, stability and translation of many mRNAs (50–52). Known constituents of SGs can be catalogued within the following categories: (i) translation factors, (ii) mRNAs, (iii) mRNA-binding proteins with roles in the regulation of translation and/or mRNA stability, (iv) proteins linked with mRNA metabolism and (v) signaling proteins with no known links with RNA metabolism (53). Expression of TDRD3 deletion mutants in HeLa cells revealed that its Tudor domain is both required and sufficient for its localization to SGs. Pull down experiments using its isolated Tudor domain led to the identification of five interacting proteins with known functions in various aspects of RNA handling. Strikingly, we show that two of them, DEAD/H box-3 (an RNA helicase also known as DDX3X/Y, DBX/Y, HLP2 and DDX14) and SERPINE1 mRNA-binding protein 1 (SERBP1), also localize to SGs following sodium arsenite treatment. Taken together, our results place TDRD3 in complexes with at least two proteins implicated in human genetic diseases (FMRP and DDX3) and suggest a role for arginine methylation in the regulation of SG dynamics.

## RESULTS

### TDRD3 is a novel modular protein

Data obtained from the UCSC Genome Browser (human Mar. 2006 hg18 assembly; NCBI Build 36.1) revealed that the human *TDRD3* gene consists of 14 exons spanning a region of ∼176.5 kb of genomic DNA on chromosome 13q21.2 (Fig. 1A). All splicing junctions conform to the GU-AG general consensus and the resulting mRNA is ∼2.9 kb in length (Fig. 1B). The *TDRD3* mRNA sequence found in databases (GenBank accession no. NM_030794) contains 10

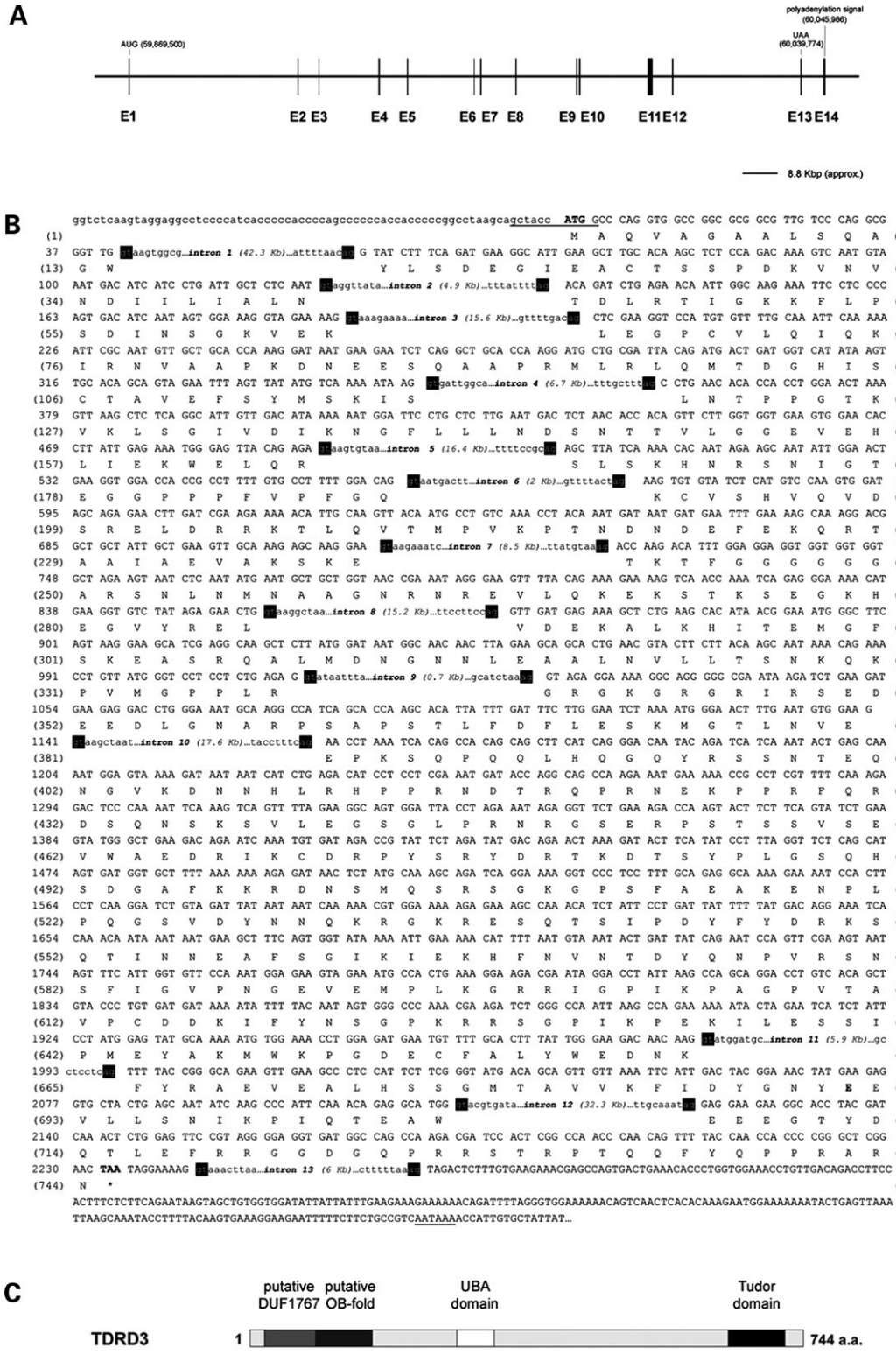


**Figure 1.** Genomic organization of the human TDRD3 locus and schematic representation of the TDRD3 protein. Analysis of the human TDRD3 gene locus revealed 14 exons spanning over ~176.5 kb of genomic DNA, encoding a 2.9-kb mRNA transcript (**A**). The sequence of exons is displayed with capital letters above the amino acid sequences they encode. Only short sequences around the intron boundaries are shown with small letters. All of the exon-intron junctions (shown in black boxes) conform to the GU-AG general consensus. The start and stop codons are in bold, whereas the Kozak sequence and the polyadenylation signal are underlined. Both nucleotides and amino acids are numbered starting from the ATG codon (**B**). The encoded TDRD3 protein consists of 744 amino acids arranged in a modular fashion. Data obtained from the NCBI Conserved Domains and the Protein Family (Pfam version 22.0) databases predict the presence of three structural domains in TDRD3: a DUF1767/OB-fold (amino acids 13–169), a UBA (amino acids 286–328) and a Tudor (amino acids 651–710) domain (see text for details) (**C**).

coding exons (exons 4–13 in Fig. 1A) with the ATG initiation codon (here designated as M94) located within exon 4. The *TDRD3* transcript derived from our analysis of the human genomic sequence (GenBank accession no. EU643838), with reference to reported cDNAs and expressed sequence tags, unveiled an additional upstream in-frame initiation codon within the first exon. The sequence preceding this new ATG (M1) is a better match to the Kozak consensus sequence (54) than the previously proposed initiation codon (Fig. 1B). This extended *TDRD3* coding sequence therefore contains three additional coding exons (1–3) upstream of the previously described exons 4–13. The STOP codon (TAA) falls within exon 13 and the polyadenylation signal (AATAAA) is located in the non-coding exon 14 (Fig. 1A and B). The presence of these upstream exons in the mRNA coding sequence was confirmed by RT–PCR and subsequent sequencing using total RNA from HeLa cells.

The predicted TDRD3 protein consists of 744 amino acids and has a calculated molecular weight of 82.7 kDa (GenBank accession no. ACC94142). Amino acid sequence similarity analysis provided by the NCBI Conserved Domains and the Protein Family (Pfam version 22.0) databases suggests that TDRD3 is a modular protein (Fig. 1C). In addition to its Tudor domain (amino acids 647–710), which selectively recognizes arginine-methylated motifs in proteins (17), TDRD3 also contains an UBA domain (amino acids 286–328), a motif found in several proteins having connections to ubiquitin and the ubiquitination pathway (49). Moreover, while searching for proteins sharing homologies with the Bloom's syndrome-associated polypeptide 75 (BLAP75) protein, Yin and colleagues identified a putative OB-fold in the N-terminal region of TDRD3 (amino acids 94–169) (55). OB-folds are compact structural motifs usually formed of five β-sheets that are often used for nucleic acid recognition, although they have also been observed at protein–protein interfaces (56). This search, however, was limited to the 'truncated' TDRD3 sequence available in databases. A new search within the Pfam database using full-length TDRD3 amino acid sequence revealed that its OB-fold is associated with another putative motif, the DUF1767 domain (amino acids 13–95). This eukaryotic domain has no known function, but is often found at the N-terminus of a nucleic acid-binding motif (Pfam number PF08585). The modular domain structure of TDRD3 suggests that it may serve as an adaptor molecule for various signaling pathways.

## TDRD3 intracellular distribution

In order to characterize the TDRD3 protein, a rabbit polyclonal antibody was raised against a synthetic peptide [coupled to keyhole limpet hemocyanine (KLH)] corresponding to the last 22 C-terminal amino acids of TDRD3 ($^{723}$DGQPRRSTRP TQQFYQPPRARN$^{744}$). The affinity-purified antibody recognized a single band of ∼83 kDa on immunoblots (IB) performed using HeLa cell extracts (Fig. 2A, lane 1), which corresponds to the predicted molecular weight of TDRD3. Immunoreactivity to endogenous TDRD3 in western blots was completely abolished by preincubation of TDRD3 antibodies with the antigenic peptide, but not with an unrelated peptide, demonstrating the specificity of our antibody (Fig. 2A, compare lanes 2 with 3). To further confirm that our antibodies specifically recognize the TDRD3 protein, *in vitro* coupled transcription/translation (IVTT) reactions were programmed with a construct designed to produce a hexahistidine-tagged truncated version of TDRD3 (ΔN328 in Fig. 5A), which still contains the reactive epitope. This TDRD3 C-terminal domain was effectively recognized by our TDRD3 antiserum in western blot analysis of the programmed IVTT reactions but not in control reactions (Fig. 2B, compare lanes 2 with 1), confirming that our antibody recognizes the TDRD3 protein sequence. Interestingly, the antibody also specifically recognized a single band corresponding to TDRD3 predicted molecular weight in the rabbit reticulocyte lysates, suggesting that TDRD3 is found endogenously in these lysates (Fig. 2B, lanes 1 and 2).

We next performed indirect IF microscopy with our polyclonal antibody in HeLa cells to examine the subcellular distribution of endogenous TDRD3. In most cells, TDRD3 staining was detected as being predominantly cytoplasmic and weakly nuclear diffused. In the cytoplasm, the fluorescent signal was generally more intense in the perinuclear region, while gradually decreasing towards the edge of the cytoplasm (Fig. 2Ca), a staining pattern reminiscent of proteins associated with polyribosomes and/or the endoplasmic reticulum. Again, preincubation of the affinity-purified antibody with an increasing amount of the immunogenic peptide resulted in a gradual decrease in the intensity of the IF signal, demonstrating the specificity of the observed staining pattern (Fig. 2Cb–e).

In order to confirm the observed TDRD3 subcellular distribution, we fractionated HeLa cells using the Qproteome Nuclear Protein Kit (Qiagen). Total proteins from each fraction were resolved by SDS–PAGE and immunoblotted with our TDRD3 antibodies, as well as with nuclear (ewing sarcoma, EWS) and cytoplasmic (GAPDH) marker antibodies to assess the efficiency of our fractionation (Fig. 2D, top). Relative abundance of TDRD3 in each fraction was determined by quantification of band intensity using the *ImageJ* version 1.37 software and expressed as a percentage of the total signal intensity obtained from all of the fractions. Although detectable in the nuclear and nuclear insoluble fractions (37%), TDRD3 was found predominantly associated with the cytosolic fraction (63%) (Fig. 2D, bottom), which correlated well with the subcellular distribution observed by IF. Taken together, these observations suggest that TDRD3 is found predominantly in the cytoplasmic compartment.

## TDRD3 is a novel component of cytoplasmic SGs

In an attempt to identify in which cellular structures TDRD3 specifically localizes to in the cytoplasm, we transfected HeLa cells with commercially available pECFP vectors encoding the enhanced cyan fluorescent protein fused to either an endoplasmic reticulum (pECFP-ER), a Golgi apparatus (pECFP-Golgi) or a mitochondrial targeting sequence (pECFP-Mito). The cells were fixed and indirect IF staining was performed using TDRD3 antibodies. Surprisingly, TDRD3 was found concentrated in cytoplasmic granule-like foci in most transfected cells (data not shown), which led us

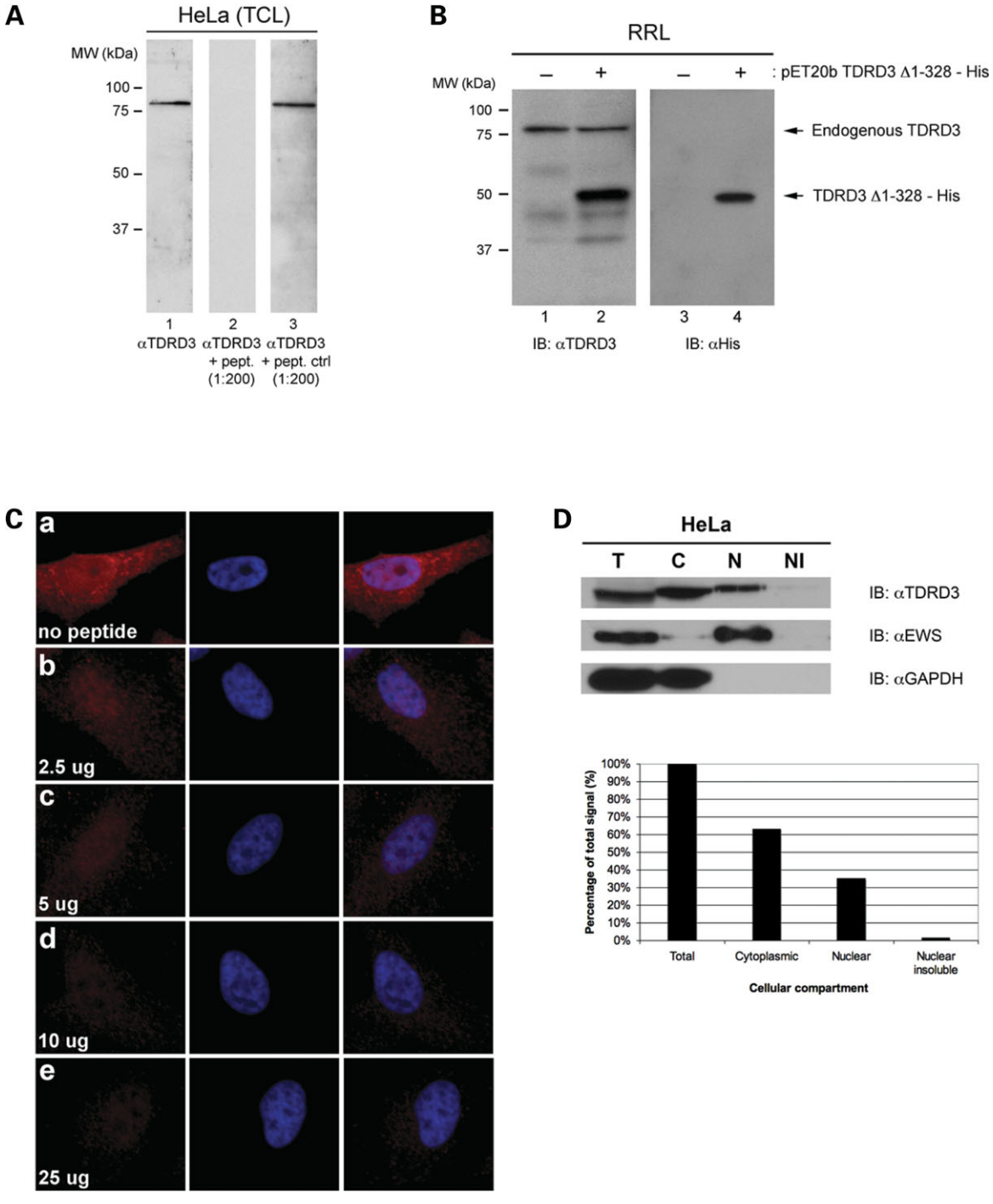


**Figure 2.** A polyclonal antibody against the novel TDRD3 protein. A HeLa total cell extract was immnublotted using our affinity-purified anti-TDRD3 polyclonal antibody (lane 1). Alternatively, immunoblots were performed using the TDRD3 antibody preincubated with a 200-fold molar excess of either the antigenic peptide (lane 2) or an unrelated peptide (ctrl; lane 3) (**A**). *In vitro* transcription and translation reactions were programmed to express a hexahistidine-tagged truncated version of TDRD3 (ΔN328). Control (−) and programmed (+) reactions were resolved by SDS–PAGE, transferred to a PVDF membrane, and immunoblotted with either TDRD3 (lanes 1 and 2) or His (lanes 3 and 4) antibodies (**B**). Actively growing HeLa cells were labeled for immunofluorescence with our TDRD3 antibody (a). Alternatively, TDRD3 antibodies were preincubated with an increasing amount (2.5–25 g) of the immunogenic peptide for 1 h on ice prior to immunofluorescence staining (b–e) (**C**). HeLa cells were fractionated using the Qproteome Nuclear Protein Kit (Qiagen). 2.5% of each fraction was resolved by SDS–PAGE, transferred to PVDF and immunoblotted with affinity-purified anti-TDRD3. Cellular fractionation efficiency was assessed using antibodies against the nuclear protein EWS and the cytoplasmic protein GAPDH. Total (T), cytoplasmic (C), nuclear (N) and insoluble nuclear protein (NI) fractions are shown (top). Quantification of the relative abundance of TDRD3 in each fraction is presented in a bar graph (bottom) (**D**).

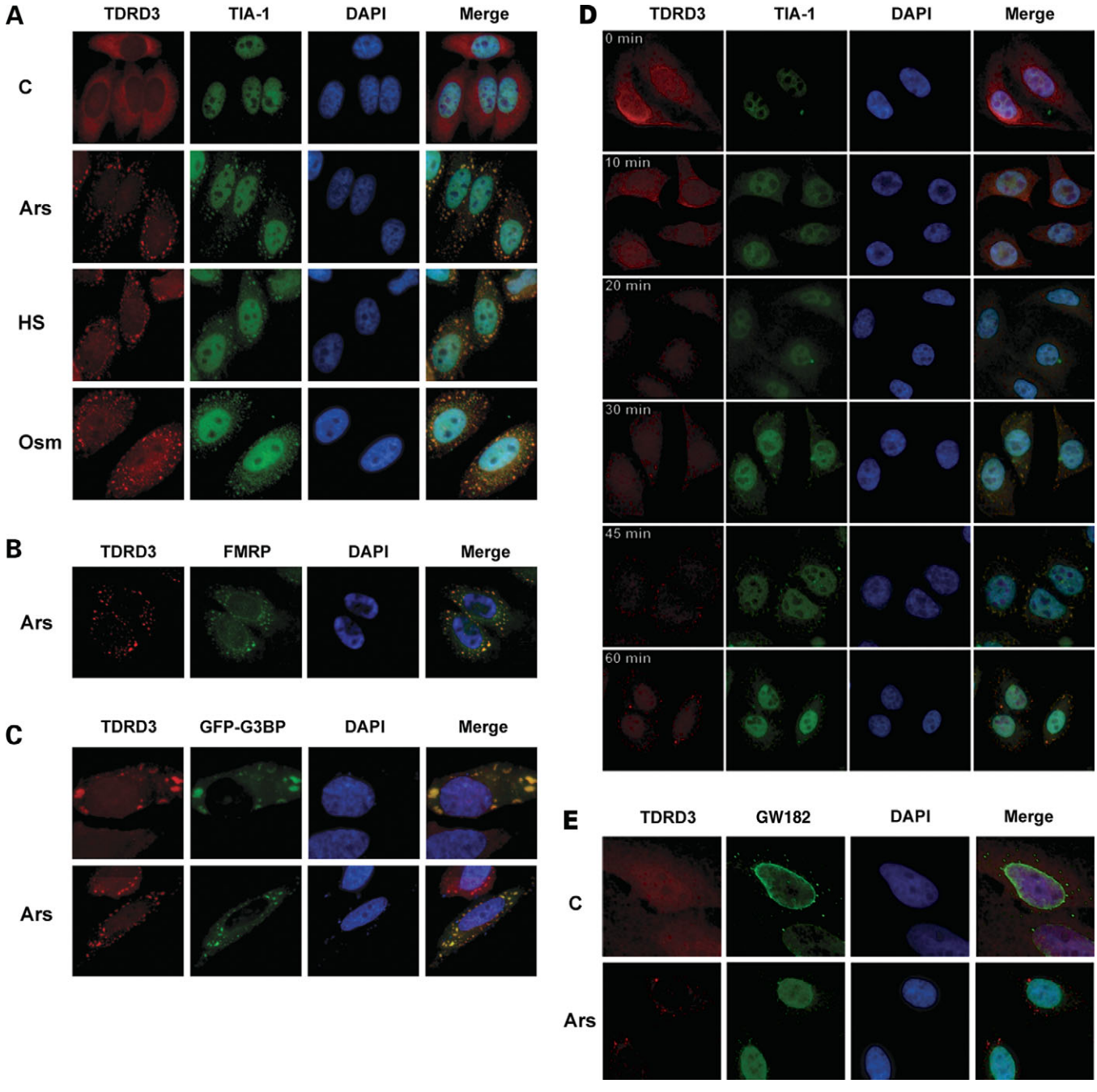


**Figure 3.** TDRD3 localizes to cytoplasmic stress granules during stress response. HeLa cells cultured on glass cover slips were left untreated (C) or exposed to oxidative stress (Ars; 0.5 mM sodium arsenite for 30 min), heat shock (HS; 43°C for 30 min) or high-osmolarity medium (Osm; 1 M sorbitol in DMEM for 1 h followed by a 30-min recovery in normal DMEM). The cells were fixed and immunostained with TDRD3 and TIA-1 antibodies to detect the endogenous proteins (**A**). Cells were stressed with 0.5 mM sodium arsenite (Ars) for 30 min, followed by immunostaining of both TDRD3 and FMRP endogenous proteins (**B**). To visualize G3BP, a GFP fusion construct was transfected into cells 24 h prior to immunofluorescence analysis. Cells were left untreated (C) or exposed to oxidative stress (Ars) for 30 min, followed by immunostaining for endogenous TDRD3 (**C**). Cells were stressed with 0.5 mM sodium arsenite for the indicated time length before their fixation and double immunofluorescence with TDRD3 and TIA-1 antibodies (**D**). HeLa cells were either left untreated (C) or stressed for 30 min with 0.5 mM sodium arsenite (Ars). After fixation, endogenous TDRD3 and GW182 (a marker of P-bodies) were detected by fluorescence microscopy (**E**).

to hypothesize that these cellular foci might be resulting from transfection-induced stress.

In order to confirm the identity of these TDRD3-containing foci, HeLa cells were exposed to different stress stimuli and double IF experiments were performed using TDRD3 antibodies in combination with an antibody directed against the RNA-binding protein TIA-1, a well-accepted marker of cytoplasmic SGs. Upon oxidative, heat and osmotic shocks, endogenous TDRD3 was redistributed to cytoplasmic SGs, where it colocalized with TIA-1 (Fig. 3A). For simplicity,

sodium arsenite was used in all subsequent experiments to induce cellular stress response. The FMRP is another protein that is well-known to relocalize to SGs (57,58), and it was recently found to interact with TDRD3 (U. Fischer, personal communication). Accordingly, colocalization of TDRD3 and FMRP into SGs following stress was also observed (Fig. 3B). Relocalization of TDRD3 in SGs was further confirmed by its colocalization with a GFP fusion of another component of these granules, the RNA-binding protein G3BP (Fig. 3C, bottom, Ars). G3BP overexpression is known to induce the formation of SGs, even in the absence of any other stress stimuli (59), and as anticipated, TDRD3 was also observed in G3BP-induced SGs (Fig. 3C, top, C). Importantly, TDRD3 was detectable in SGs as early as 10 min following sodium arsenite treatment (Fig. 3D), which is comparable to the kinetics of TIA-1 relocalization to SGs (60). However, the use of finer live cell imaging approaches will be required to determine the precise kinetics of TDRD3 recruitment to SGs. Finally, TDRD3 did not localize to other cytoplasmic mRNA foci, such as processing bodies, as shown by the absence of colocalization with GW182 (Fig. 3E), an RNA-binding protein resident of these structures (61,62). Taken together, our results indicate that TDRD3 is a novel component of cytoplasmic SGs.

## TDRD3 is associated with translating polyribosomes

SGs are considered to be stalled aggregates of 48S preinitiation complexes and contain a number of translation factors, including eIF3, eIF4E, eIF4G, PABP-1 and FMRP (50). In contrast to TIA-1, which is not normally associated with the translational machinery (63), FMRP can be found on polyribosomes (64,65). To determine if TDRD3 is associated with translational complexes, post-nuclear supernatants were subjected to velocity sedimentation through sucrose gradients and each collected fraction was analyzed by western blot for the presence of TDRD3 (Fig. 4, control panels). Using this protocol, it is possible to resolve free ribosomal subunits (40S and 60S) and monomers (80S) from actively translating polysomes, which sediment towards the bottom of the gradient, as confirmed by the distribution of the ribosomal S6 protein in each fraction (Fig. 4, S6 panel). Strikingly, TDRD3 was found distributed in both the light and the heavy sedimenting fractions of the sucrose gradient, following a pattern similar to what is observed for FMRP (Fig. 4, respective panels). Heat shock protein 72 (Hsp72) was used as a negative control in these experiments as it should not be associated with ribosomes. These results indicate that TDRD3 is associated with actively translating polyribosomes in cycling HeLa cells.

Under stress conditions such as heat shock or arsenite, FMRP shifts away from polyribosomes, which are largely disassembled due to inhibition of translation initiation (50,57,58,66). Thus, we next determined if TDRD3 would follow the same pattern in ribosome profiles following stress induced by arsenite treatment (Fig. 4, Arsenite panels). HeLa cells were incubated with sodium arsenite as above, before being subjected to velocity sedimentation through sucrose gradients. Each collected fraction was then analyzed by western blot for the presence of TDRD3. As expected,

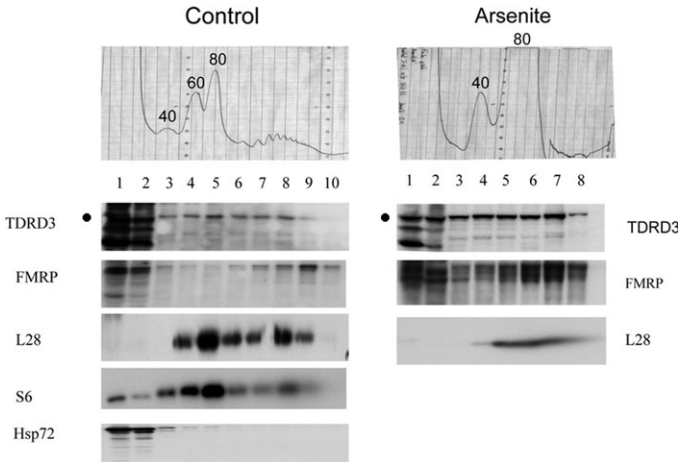


**Figure 4.** TDRD3 is associated with polyribosomes in HeLa cells. Cytoplasmic extracts were prepared from HeLa cells grown in normal conditions and centrifuged on a 10–60% w/w linear sucrose gradient. Fractions were collected and analyzed by western blot with antibodies against the ribosomal S6 protein and FMRP (as positive controls), TDRD3, and Hsp72 (as a negative control) (Control panel). Cytoplasmic extracts from HeLa cells treated with 0.5 mM sodium arsenite for 30 min were analyzed in parallel and the collected fractions were analyzed by western blot using the ribosomal L28 protein as positive control (Arsenite panel). Fractions from the top to the bottom of the gradient are shown from left to right. The positions of free small (40S) and large (60S) ribosomal subunits, monosomes (80S), and polysomes are indicated in each profile. The band corresponding to TDRD3 is indicated by a 'dot' on the side of the respective panels. Additional bands detected on the immunoblots represent non-specific reactivity with our polyclonal antibody.

polysome peaks were almost undetectable following arsenite treatment, and this was associated with an increase of the 80S monomer fraction (Fig. 4, Arsenite UV profile). Under these stress conditions, the bulk of TDRD3 was found mainly associated with monomeric ribosomes and lighter fractions, again following the pattern previously reported for FMRP (Fig. 4, respective panels). Taken together, these results suggest that TDRD3's function may be at the level of translational regulation.

## The Tudor domain is both essential and sufficient for TDRD3 translocation to cytoplasmic SGs

To identify which part of TDRD3 was important for its localization to SGs, a series of myc epitope-tagged deletion constructs was generated (Fig. 5A). The fusion proteins were expressed in HeLa cells and IF microscopy was performed using myc antibodies (Fig. 5B and E). As its endogenous counterpart, full-length myc-tagged TDRD3 localized predominantly to the cytoplasm with a weaker diffuse nuclear staining (Fig. 5Ba). Overall, the intracellular distribution patterns of deletion mutants were similar to that of full-length TDRD3 (Fig. 5Bb–e), although a certain degree of variation was observed depending on expression levels. A second series of constructs was engineered to express specific conserved domains of the TDRD3 protein (Fig. 5A). The predicted molecular weight of these myc-tagged TDRD3 isolated domains ranges from 4 to 36 kDa, which means that they are likely to diffuse freely between the cytoplasm and

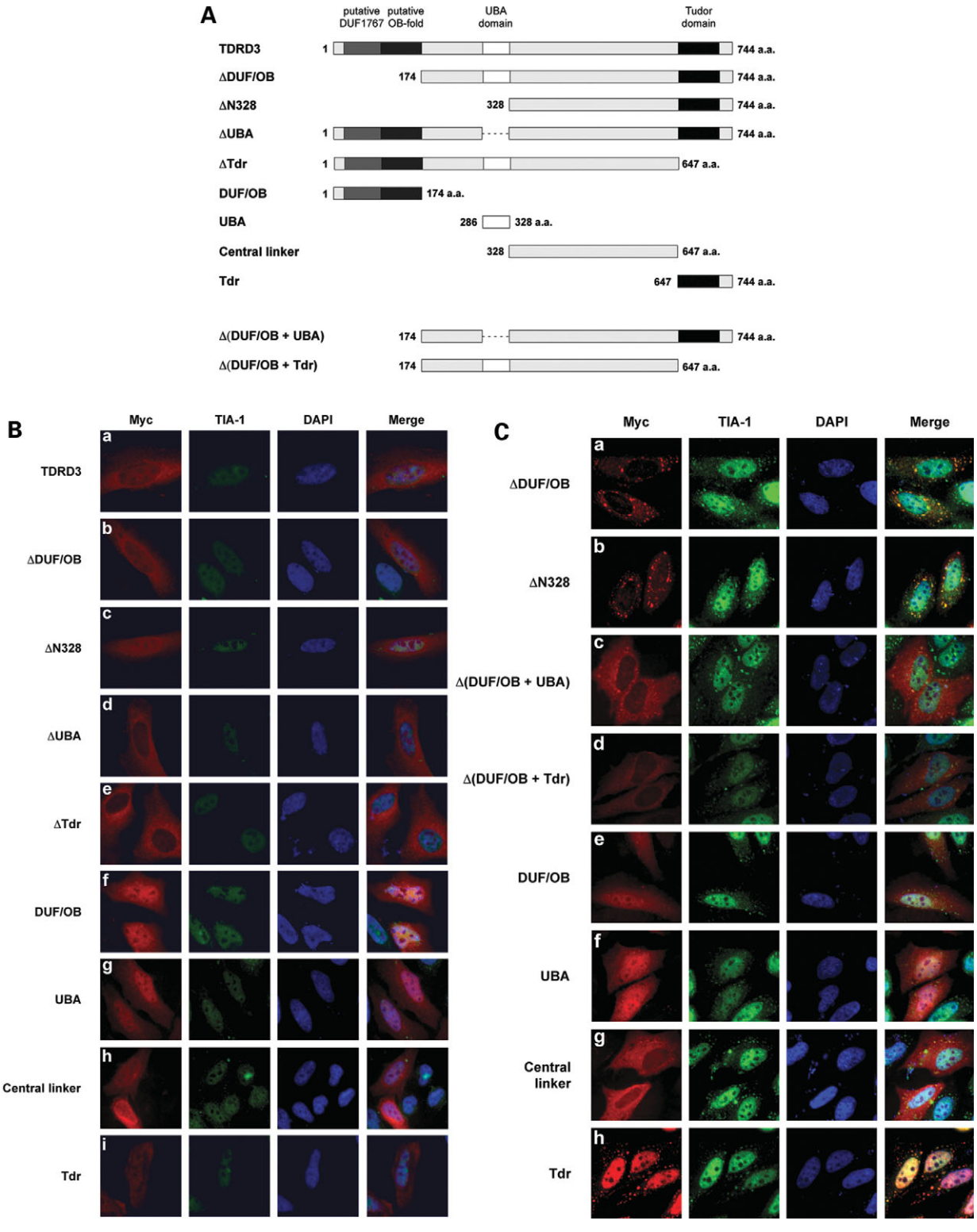


**Figure 5.** The Tudor domain of TDRD3 is both required and sufficient for its recruitment to stress granules. Diagram showing the various myc epitope-tagged TDRD3 deletion mutants used in this study (**A**). HeLa cells were transiently transfected with each deletion mutant. Twenty-four hours post-transfection, cells were left untreated and labeled for immunofluorescence with TIA-1 and myc antibodies to detect endogenous TIA-1 protein and recombinant myc-tagged proteins (**B**). Alternatively, transfected cells were treated with 0.5 mM sodium arsenite for 30 min. Indirect immunofluorescence staining was performed as described above (**C**). HeLa cells were transiently transfected with constructs expressing recombinant myc-tagged Tudor domain of SMN, SPF30 or TDRD3. Twenty-four hours post-transfection, cells were treated with 0.5 mM sodium arsenite for 30 min. Indirect immunofluorescence staining was performed using myc and TIA-1 antibodies (**D**). Total cell lysates of HeLa cells transiently expressing myc-tagged TDRD3 deletion mutants, as well as SMN and SPF30 Tudor domains, were immunoblotted with myc antibodies to confirm expression (**E**).

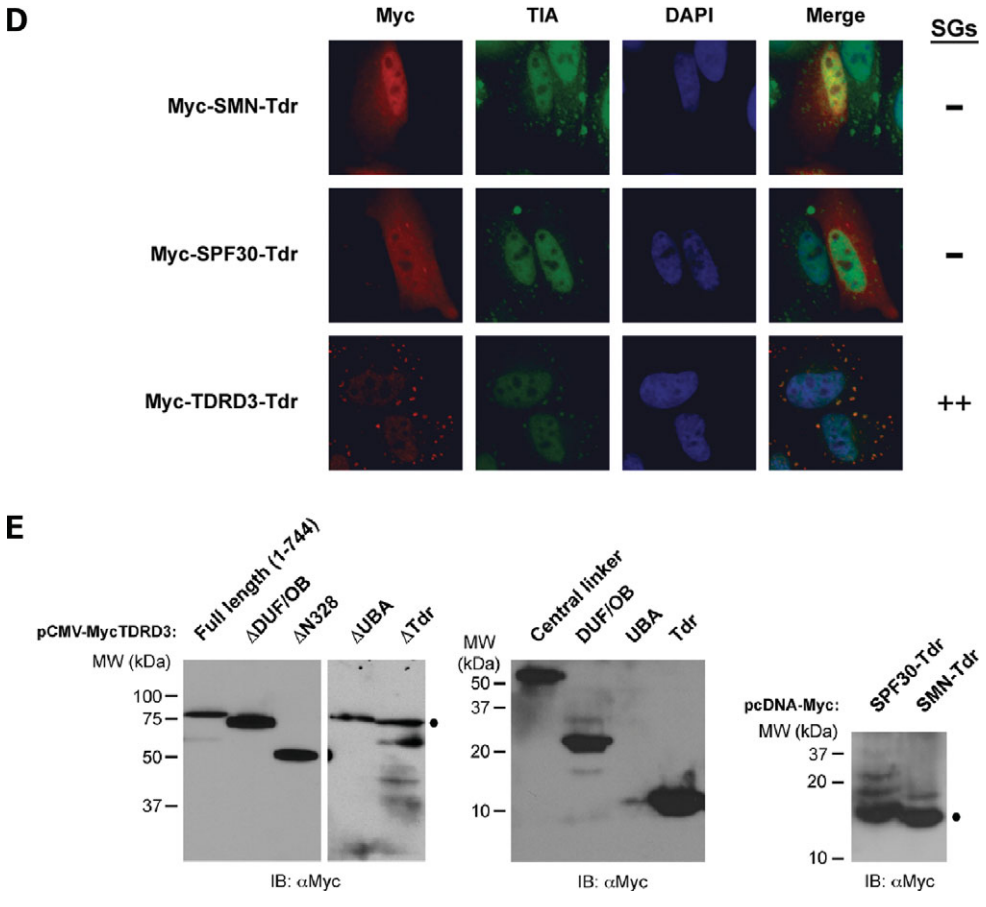


**Figure 5.** Continued.

the nucleus. As expected, expression of TDRD3's isolated domains in HeLa cells resulted in both cytoplasmic and nuclear diffused staining (Fig. 5Bf–i). Finally, in contrast with G3BP, overexpression of TDRD3 (or any deletion mutant) did not significantly induce the formation of SGs in the absence of external stress stimuli. Taken together, these experiments did not permit the clear identification of a domain influencing normal TDRD3 subcellular localization.

We next assessed whether each TDRD3 deletion mutant had retained the property of being relocalized to cytoplasmic SGs following sodium arsenite treatment (Fig. 5C). Intriguingly, overexpression of any myc-tagged TDRD3 proteins harboring the DUF1767/OB-fold motifs was toxic for cells when they were put under stress conditions. In order to circumvent this problem, we generated additional deletion mutants of TDRD3, lacking the N-terminal DUF1767/OB-fold domains [Fig. 5A; TDRD3 Δ(DUF/OB+UBA) and TDRD3 Δ(DUF/OB+Tdr)]. These mutants displayed an intracellular distribution that was identical to their respective N-terminal-containing counterparts in the absence of stress (data not shown). Following arsenite treatment, ΔDUF/OB, ΔN328 and Δ(DUF/OB+UBA) all still relocalized to SGs, albeit to varying degrees (Fig. 5Ca–c). In contrast, Δ(DUF/OB+Tdr) was not detectable in cytoplasmic SGs following stress stimuli (Fig. 5Cd), which suggest a requirement for the Tudor domain in this process. Accordingly, when TDRD3's isolated domains were tested, only the Tudor domain (Tdr) was found to be sufficient for relocalization to SGs upon arsenite treatment (Fig. 5Ce–h). Interestingly, the central linker fragment (amino acids 328–647) was redistributed almost entirely to the cytoplasm following arsenite treatment (compare Fig. 5Bh with 5Cg), suggesting that this region may contain an element favoring its export from the nucleus to the cytoplasm upon stress. Taken together, these results show that the Tudor domain of TDRD3 is both required and sufficient for its recruitment to cytoplasmic SGs during cellular stress response, although the central linker region may also contribute to this process by promoting nuclear-cytoplasmic translocation.

SMN, which also harbors a Tudor domain, was previously reported to relocalize to SGs upon stress (67). Hence, we next wanted to determine whether this feature was unique to the Tudor domain of TDRD3 or common to other known Tudor domains. To investigate this possibility, HeLa cells were transiently transfected with the isolated Tudor domain of SMN, SPF30 or TDRD3 fused to a myc epitope tag (Fig. 5D and E). Twenty-four hours post-transfection, cells were treated with sodium arsenite and immunostained with myc antibodies. The Tudor domain of TDRD3 was effectively recruited to SGs upon stress (Fig. 5D). However, neither SMN nor SPF30's Tudor domain localized to SGs under the same conditions (Fig. 5D). These observations therefore suggest

**Table 1.** Potentially methylated proteins involved in RNA processing interact with the Tudor domain of TDRD3

| MW SDS–PAGE | Protein name (GenPept acc. no) | Score | RG-motifs | Known or putative function(s)[a] | Calc. mass (kDa) |
|---|---|---|---|---|---|
| p80 | Ewing sarcoma breakpoint region 1 (NP_005234) | 70.26 | 19× RGG<br>$^{300}$RGRGRGG$^{306}$<br>$^{314}$RGGRGGGRGG$^{323}$ | RNA-binding protein (transcription and pre-mRNA splicing machineries) | 68.592 |
| p75 | DEAD/H box-3 (NP_001347) | 40.17 | 10× RG<br>$^{121}$RGG$^{123}$ | RNA splicing and transport | 73.244 |
| p60 | Fus (NP_004951) | 40.15 | 2× RGG<br>$^{216}$RGGRGRG$^{222}$<br>$^{245}$RGRGGGRGGRGG$^{256}$<br>$^{380}$RGGGNGRGGRG<br>RGGPMGRGG$^{399}$<br>$^{475}$RRGGRGGYDRGGYRGRGG<br>DRGGFRGGRGGGDRGG$^{508}$ | RNA splicing and nuclear/cytoplasmic shutting | 53.377 |
| p50 | Eukaryotic translation elongation factor 1 alpha 1 (NP_001393) | 150.19 | 2× RG | Translation anchoring | 50.141 |
| p35 | SERPINE1 mRNA-binding protein 1 (NP_001018077) | 60.11 | 1× RG, 1× RGG<br>$^{163}$RGRGGLGRGRG<br>GRGRGMGRG$^{182}$<br>$^{346}$RGGRGGRGGRGRGGR$^{360}$ | Regulation of mRNA stability | 44.966 |

HeLa cells were lysed and incubated with either purified recombinant GST (as a control) or GST-TDRD3-Tdr proteins coupled to glutathione-agarose (see Materials and Methods). The polypeptides specifically pulled down by TDRD3-Tdr, that were not pulled down by GST alone, were excised from the gel and sent for mass spectrometry analysis and identification. Sequencing data were analyzed using the Sequest software and only the top match obtained for each band is listed (highest score). Potentially methylated RG-rich motifs found in the amino acid sequence (GenPept database) of each protein are also depicted, as well as their known or putative function (see text for details and references).
[a]see text for reference.

that the mechanism by which TDRD3 relocalizes to SGs likely involves interactions that are mediated by, and that are unique to its Tudor domain.

### Identification of TDRD3 Tudor domain interactors

In order to begin the identification of proteins interacting specifically with the Tudor domain of TDRD3, a glutathione-*S*-transferase (GST) pull-down was performed using HeLa total cell extracts. A recombinant fusion protein was generated, consisting of GST fused to the C-terminal region of TDRD3 (amino acids 647–744) encompassing the Tudor domain (GST-TDRD3-Tdr). GST-TDRD3-Tdr and GST alone were then coupled to glutathione-agarose and used as affinity columns to pull down interacting proteins from HeLa cell lysates. The retained proteins were resolved by SDS–PAGE and stained with Coomassie Blue. GST-TDRD3-Tdr bound several polypeptides that were not bound by GST alone (data not shown). Five of these specific protein bands were excised from the gel and subjected to mass spectrometry identification (68). The top matches obtained for each band are EWS, FUS, DDX3, SERBP1 and EEF1A1 (see Table 1 for details). Remarkably, all these proteins have known roles in RNA handling, which reinforces our hypothesis that TDRD3 likely functions in post-transcriptional processes.

Interestingly, EWS was previously shown to interact with the Tudor domain of SMN (69), although arginine methylation was not a requirement for binding in this case. A *Caenorhabditis elegans* ortholog of SERBP1 was also found to interact with SMN (70). Finally, FUS is present in a complex with SMN and the NFAR proteins (71), although a direct interaction between SMN and FUS was not reported. These observations prompted us to verify if all the proteins identified in our screen were also able to bind the Tudor domain of SMN. These experiments revealed that EWS and FUS were also interacting with SMN-Tdr, but the interactions with DDX3 and EEF1A1 were specific to TDRD3 (Goulet and Côté, unpublished data). SERBP1 was not tested in these experiments. The functional relevance of each of these interactions in the context of the full-length protein will need to be addressed in future studies.

### Direct contact with methylated arginines contributes to TDRD3 relocalization to SGs

All the identified proteins also contain RG-rich motifs, which represent common target sites for protein arginine methyltransferases (Table 1). In fact, the presence of methylated arginines in EWS and FUS has been documented (6,7,72), and we have also detected modified arginines in our proteomic analysis (data not shown). Since the Tudor domain of TDRD3 can specifically recognize methylated arginine motifs in proteins (16,17), we speculated that TDRD3 might be recruited to SGs through methyl-dependent interactions with one or more of its binding partners. Previous studies have demonstrated that an E134K amino acid substitution in the Tudor domain of SMN abolished its interaction with arginine-methylated polypeptides (17). This amino acid is conserved in the Tudor domain of TDRD3 and corresponds to residue E691.

In order to determine if the equivalent E691K substitution in TDRD3 Tudor domain would also abolish its capacity to interact with methylated arginines, an *in vitro* binding assay was used, with synthetic $(RG)_4$ biotinylated peptides containing either no modified amino acids or symmetrically dimethylated arginines (sDMA). Purified recombinant GST-TDRD3-Tdr fusion proteins were incubated with the biotinylated peptides coupled to streptavidin-agarose. As previously reported (17), purified GST-TDRD3-Tdr bound to sDMA peptide columns in a dose-dependent manner, but did not bind the unmethylated peptide (Fig. 6A, compare lanes 5–7 with lanes 2–4). Remarkably, this binding was completely abolished with the introduction of the E691K mutation in the TDRD3 Tudor domain (Fig. 6A, GST-TDRD3-Tdr E691K). This result confirms that the Tudor domain of TDRD3 behaves as a methyl-binding protein module similar to that of SMN, in which the E691 residue is crucial for direct contact with dimethylated arginine motifs. This TDRD3 mutant was next used to determine if this methylarginine binding surface was important for recruitment to SGs. HeLa cells were transfected with a myc-tagged TDRD3 Tudor fragment containing the E691K point mutation. Twenty-four hours post-transfection, cells were stressed with sodium arsenite and labeled for IF with myc antibodies. Strikingly, the introduction of the E691K mutation in the Tudor domain of TDRD3 reduced its recruitment to SGs upon stress by at least 50% (Fig. 6B). This observation suggests that TDRD3's recruitment to SGs is likely mediated through specific protein–protein interactions involving methylated arginines.

In order to fulfill this role, an interacting protein would have to satisfy at least two conditions. First, the protein has to be relocalized to SGs upon stress. Second, its interaction with TDRD3 must be affected by the E691K mutation. To verify the first criteria, IF microscopy was performed using commercially available antibodies for EWS, DDX3, EEF1A1 and FUS, or an epitope-tagged version of SERBP1 (myc) (Fig. 6C). Strikingly, only DDX3 and SERBP1 relocalized significantly to SGs following arsenite treatment, while the other proteins showed little to no response to the stress stimuli (Fig. 6C, respective panels). To verify the second condition, a GST-TDRD3-Tdr pull down was performed as above using total HeLa cell lysates as input, and the retained proteins were analyzed by western blot with commercially available antibodies specific to EWS, DDX3, FUS and EEF1A1 (Fig. 6D, lane 3). The E691K mutation completely prevented the interaction with EWS and FUS, while reducing binding to DDX3 and EEF1A1 by 50 and 90%, respectively (Fig. 6D, lane 4). We have not yet assessed if the interaction of SERBP1 with TDRD3 was also affected by the presence of this mutation due to antibody availability. Taken together, these results identify DDX3 as a good candidate to mediate the recruitment of TDRD3 to SGs (or vice versa). Moreover, these experiments show that the methyl-binding surface of TDRD3's Tudor domain is important for this process.

### Arginine methylation: a general regulator of SG assembly/disassembly?

A recent study uncovered a new subset of smaller cytoplasmic foci that are clearly distinct from SGs, which contain FMRP (73). FMRP is an RG-rich protein that is an *in vitro* substrate for protein arginine methyltransferases (74). FMRP relocalizes to *bona fide* SGs following treatment with various stimuli, and it was suggested that arginine methylation may regulate its translocation from smaller cytoplasmic foci into SGs by promoting its heterodimerization with fragile X mental retardation-related protein 1 (FXR1p) (73). Since this mechanism is reminiscent of what we propose for the recruitment of TDRD3 along with DDX3 and/or SERBP1 to SGs, we wanted to determine if arginine methylation may play a general role in the assembly of SGs.

HeLa cells were grown for 20 h in the presence of 1 mM 5′-deoxy-5′-methylthioadenosine (MTA), a well-characterized general inhibitor of methylation (9). Following this pre-treatment, which reduced steady-state arginine methylation levels by ∼50% (Fig. 7C), cells were incubated with sodium arsenite and IF microscopy was performed with antibodies against TDRD3 and TIA-1 to monitor the formation of SGs. First, it was confirmed that the MTA treatment alone did not cause the formation of SGs (data not shown). As observed in non-treated HeLa cells (see time-course in Fig. 3D), TDRD3 was detectable in nascent SGs as early as 10–15 min after the addition of arsenite in mock-treated cells, and TIA-1 after ∼20 min (data not shown). SGs containing both TDRD3 and TIA-1 were present in 100% of cells after 30 min. Similarly, cells pre-treated with the methylation inhibitor MTA all contained TDRD3- and TIA-1-positive SGs after 30 min of stress stimulus, although small differences were observed at shorter time points. Specifically, recruitment of TDRD3 to SGs was delayed to some extent, while more cells with TIA-1-containing SGs could be clearly discerned after 15 min (data not shown). Thus, reducing arginine methylation levels by ∼50% did not prevent assembly of SGs, although the precise composition of these granules seemed to be altered.

Another series of stressed cells (pre-treated or not with MTA) was immunostained for TDRD3 at various time points after being returned to normal growth media. As expected from previous studies (75), SGs first decreased in number, but increased in size, and then gradually disappeared following stress withdrawal, so that they were no longer detectable after 120–150 min in mock-treated cells (Fig. 7A, DMSO panels). In contrast, the number of SG-positive cells increased by ∼6-fold in cells pre-treated with the methylation inhibitor MTA after 150 min of recovery (Fig. 7A, MTA panels, and 7B). These observations were also confirmed using TIA-1 as a SG marker (data not shown). Taken together, our experiments support a role for methylation in regulating SG dynamics and composition, potentially by regulating protein–protein interactions and impacting on SG disassembly.

## DISCUSSION

We report here the first characterization of TDRD3, a novel Tudor-containing protein associated with poor prognosis of estrogen receptor-negative breast cancers (48). Our findings identify TDRD3 as a novel component of cytoplasmic SGs, where it relocalizes following various cellular stresses, including oxidative, heat and osmotic shocks. We also show that TDRD3

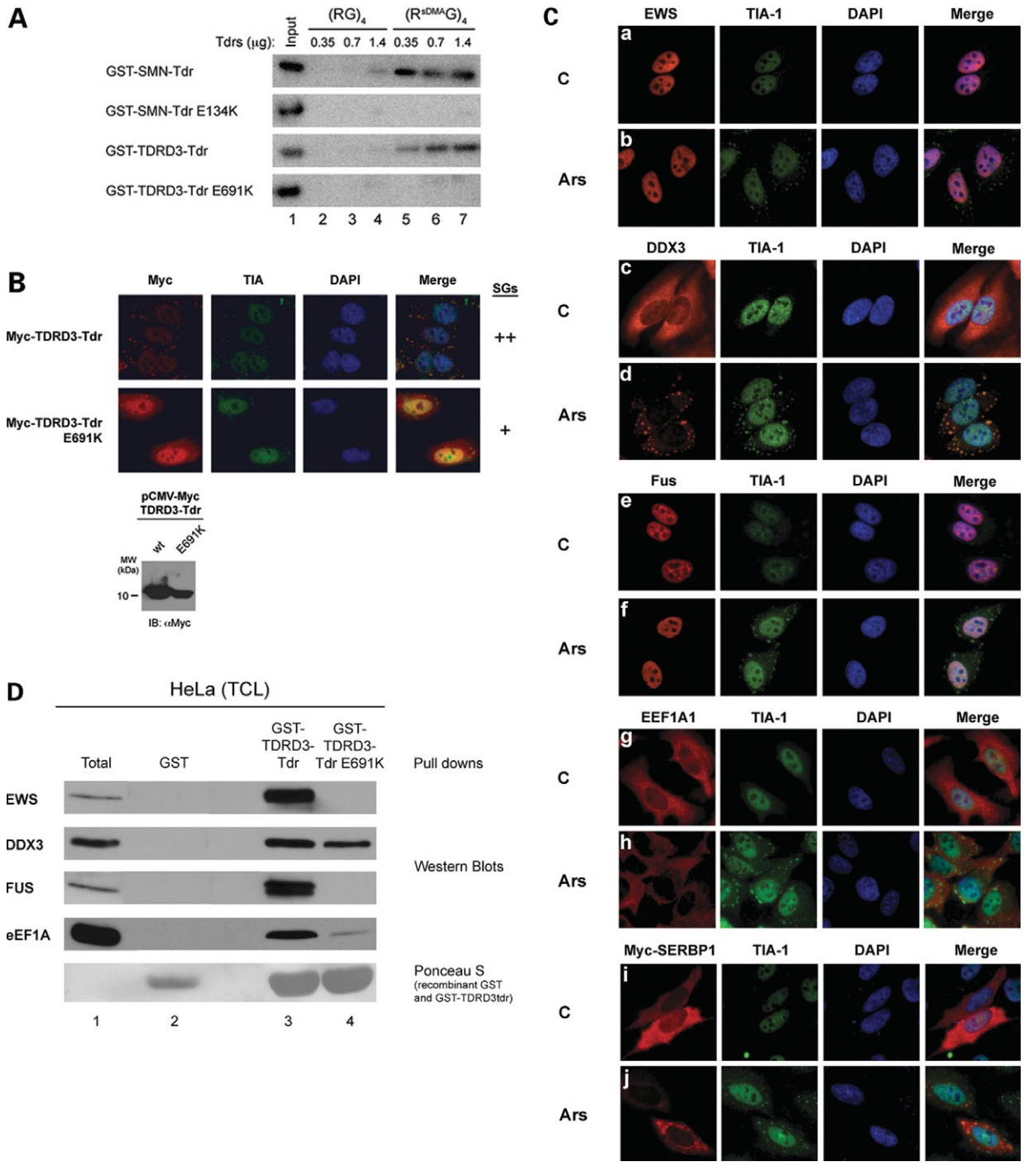


**Figure 6.** Direct contact with methylated arginines contributes to TDRD3 relocalization to SGs. Biotinylated ($RG_4$) peptides containing either unmethylated arginines or symmetrically dimethylated arginines (sDMA) were bound to streptavidin-agarose and used as affinity columns to measure the binding of purified GST fusion SMN and SMN E134K (as controls) and/or TDRD3 and TDRD3 E691K Tudor domains. The bound GST-Tdr fusion proteins were resolved by SDS-PAGE, transferred to a PVDF membrane, and detected by immunoblotting using GST antibodies (**A**). HeLa cells were transiently transfected with constructs expressing recombinant myc-tagged wild type or mutated (E691K) TDRD3 Tudor domain. Twenty-four hours post-transfection, cells were treated with 0.5 mM sodium arsenite for 30 min. Indirect immunofluorescence staining was performed using myc and TIA-1 antibodies (**B**). HeLa cells were either left untreated (C) or treated with 0.5 mM sodium arsenite for 30 min (Ars). Cells were then labeled for immunofluorescence with EWS (a and b), DDX3 (c and d), FUS (e and f), or EEF1A1 (g and h) in combination with TIA-1 antibodies to detect endogenous proteins. HeLa cells transiently transfected to express myc-tagged SERBP1 (i and j) were either left untreated (C) or stressed as described above (Ars), before being immunostained with TDRD3 and myc (SERBP1) antibodies (**C**). HeLa cells from 2× 150 mm plates were lysed and incubated with purified recombinant GST (as a control), GST-TDRD3-Tdr or GST-TDRD3-Tdr E691K proteins coupled to glutathione-agarose. The retained proteins were resolved by SDS-PAGE, transferred to PVDF, and immunoblotted with the specified antibodies to confirm mass spectrometry identifications. The membrane was stained with Ponceau Red prior to immunoblotting, in order to show the GST-fusion proteins (**D**).

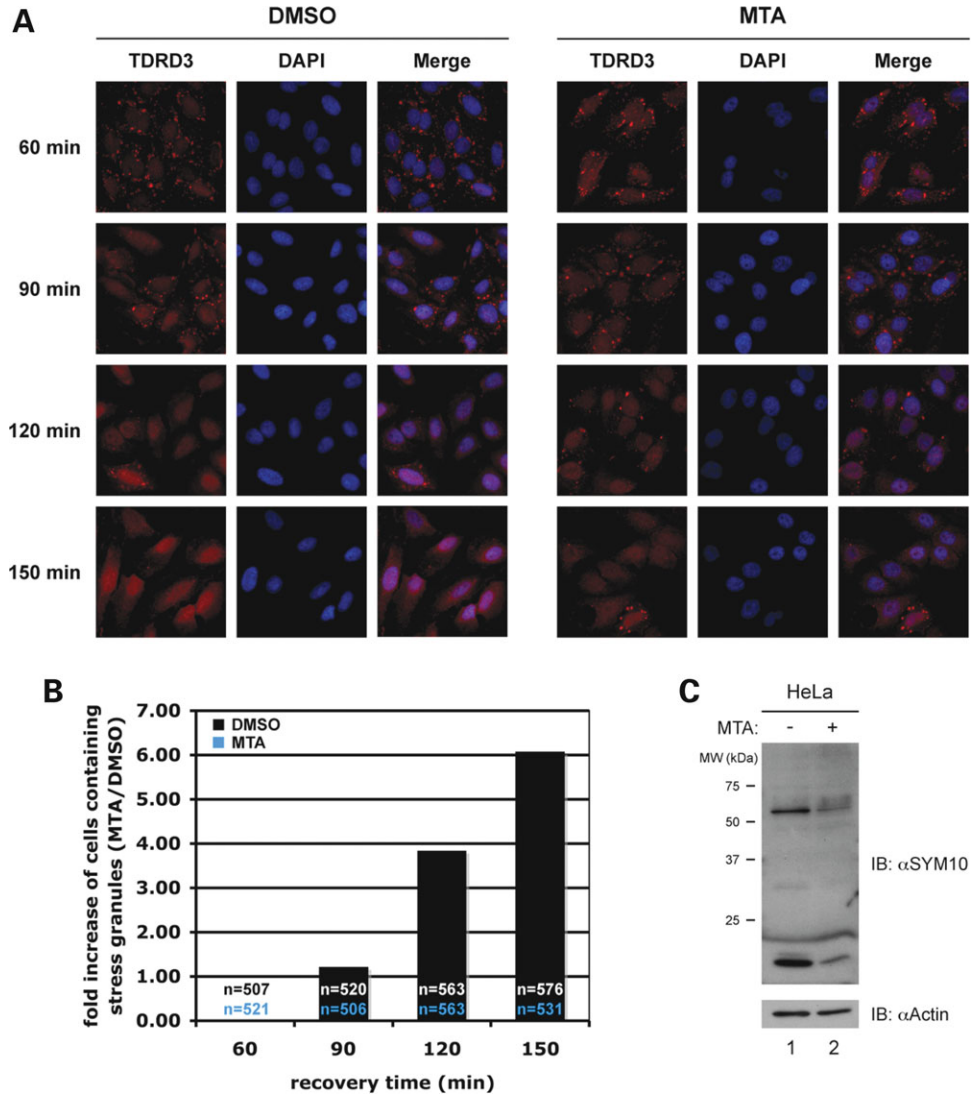


**Figure 7.** Arginine methylation and SG dynamics. HeLa cells grown on cover slips were stressed with 0.5 mM sodium arsenite for 30 min. Cells were then returned to normal growth media and prepared for TDRD3/TIA-1 immunostaining after the indicated incubation periods (**A**). The experiment was repeated twice using different batches of cells. At least 500 cells were counted for each time point and condition. Fold increase of SG-positive cells in the MTA-treated cells when compared the DMSO-treated cells is depicted in a bar graph (**B**). Cell extracts prepared from HeLa cells grown in the presence (+) or the absence (−) of the general methylation inhibitor MTA were immunoblotted with the SYM10 antibody to confirm the reduction in steady-state arginine methylation levels. The same extracts were immunoblotted with actin antibodies to control for equal loading (**C**).

follows FMRP in polysome profiles under normal and stress conditions. A proteomic screen led to the identification of five novel TDRD3 interacting partners with known or putative roles in various aspects of RNA metabolism. Moreover, all these TDRD3 interacting proteins harbor RG-rich motifs that represent consensus sites for protein arginine methyltransferases. Our experiments revealed that two of these proteins, SERBP1 and DDX3 [a gene associated with Sertoli-cell-only (SCO) syndrome], are also novel constituents of cytoplasmic SGs. The Tudor domain of TDRD3 was both required and sufficient for its relocalization to SGs. Specifically, the use of a conserved mutation helped us demonstrate that the methyl-binding surface in the Tudor domain of TDRD3 is involved in this process. Finally, we found that arginine methylation may be a general regulator of SG dynamics and protein composition.

## TDRD3 is a novel component of cytoplasmic SGs

We report here that the novel Tudor-containing protein TDRD3 relocalizes with TIA-1, a well-known SG marker upon arsenite treatment, heat shock and osmotic shock (Fig. 3A). TDRD3 also colocalized in SGs with FMRP following arsenite treatment, and it can be recruited to transfection-induced SGs upon GFP-G3BP overexpression (Fig. 3B and C, respectively). In contrast, TDRD3 did not colocalize with processing body (also known as GW bodies) markers under any conditions tested here (Fig. 3E and data not shown). TIA-1 is considered to be a crucial mediator of SG assembly, as it is thought to promote aggregation through its prion-like glutamine-rich C-terminal domain (60). FMRP is also thought to participate, along with TIA-1,

in the 'primary aggregation/nucleation' phase of SG assembly (50). Since we found that TDRD3 can be detected in SGs concomitantly or even prior to TIA-1 (Fig. 3C), it may participate in the early phases of SG assembly. This is also consistent with the association of TDRD3 with polyribosomes (Fig. 4), since SG assembly involves stalled translation initiation complexes, polysome disassembly and mRNP aggregation (50). However, TDRD3 did not significantly induce SG formation on its own in the absence of additional stress stimuli, in contrast to TIA-1, G3BP and FMRP, which are all thought to physically nucleate SG assembly (50). In fact, our experiments suggest that TDRD3 may participate in the SG disassembly process by engaging in protein–protein interactions regulated by arginine methylation (see below), although further experiments will be required to fully confirm this hypothesis.

### TDRD3 interacts with proteins involved in RNA handling and/or metabolism

We have uncovered, using a large-scale Tudor domain pull down approach, five novel protein-binding partners for TDRD3 (Table 1). Strikingly, we found that two of these proteins, SERBP1 and DDX3, also relocalize to SGs following sodium arsenite treatment, although we cannot rule out that some of the other TDRD3 binding partners may still transiently associate with SGs (Fig. 6C). In addition, each of the newly identified TDRD3 interactors has previously been linked with post-transcriptional regulatory processes. EEF1A1 is a translation initiation factor that has been shown to participate in the anchoring of specific mRNAs to the cytoskeleton (76), while DDX3 has been implicated in pre-mRNA splicing, nuclear export, mRNA transport and translation initiation (77–85). TDRD3 also interacts with FMRP and associates with translating polyribosomes. Taken together, these observations strongly suggest that TDRD3 may function as a translational regulator.

In contrast, SERBP1 (a.k.a. PAI-RBP1) has been suggested to play a role in mRNA stability (86), while EWS and FUS have both been implicated in alternative splicing regulation (87–93). Intriguingly, TDRD3 has been identified in a proteomic screen of proteins associated with spliceosome complexes (94). However, our experiments did not provide any indications to support a role for TDRD3 in splicing (Goulet and Côté, unpublished data). Further experimentation will be needed to establish its function in this precise mechanism.

### The Tudor domain of TDRD3 is both required and sufficient for its localization to SGs

All the proteins identified in our GST-TDRD3-Tdr pull down are either known or are very likely to contain methylated arginines (Table 1). This is consistent with our previous studies, which demonstrated that the Tudor domain of TDRD3 can specifically recognize methylated arginine motifs in proteins (17). Since DDX3 and SERBP1 are the only proteins that could be detected in SGs, these proteins are good candidates to mediate the methyl-dependent recruitment of TDRD3 to these structures. In this study, we have presented several evidences supporting this model. First, thorough deletion mapping clearly showed that the Tudor domain of TDRD3 is both sufficient and required for its localization to SGs, although the central linker region may also contribute to this process by promoting nuclear-cytoplasmic translocation (Fig. 5). Second, a single E->K substitution (E691K) in the methylarginine-binding interface of TDRD3's Tudor domain is sufficient to greatly reduce its recruitment to SGs (Fig. 6B). Third, this same E691K mutation also reduces the interaction with DDX3 (Fig. 6D). Finally, general methylation inhibitors perturbed the dynamics of SG assembly/disassembly as well as their composition (Fig. 7 and see below).

### Arginine methylation and SG dynamics

A simple prediction from our model would have been for methylation inhibitors to prevent or at least reduce the recruitment of TDRD3 to SGs, potentially even preventing their formation. In contrast, our results show that MTA treatment did not prevent SG assembly, as 100% of cells contained a normal number of SGs 30 min after arsenite treatment (data not shown). However, we cannot eliminate the possibility that a 50% reduction in overall arginine methylation may not be sufficient to observe a drastic effect. Moreover, our estimate of the efficiency of the MTA treatment does not take into account the different turnover rate of all the proteins that could be involved in SG assembly. Nevertheless, we did observe a tendency for TDRD3 and TIA-1 to no longer follow the same kinetics of recruitment as seen at early time points of SG formation. SGs are highly dynamic structures with components rapidly and continuously shuttling in and out (75). Hence, more in-depth studies using Fluorescence Recovery After Photobleaching experiments or similar approaches would be required to confirm and quantify these effects. Following the same idea, a longer time window may explain why we were able, under the same conditions of MTA treatment, to observe more profound differences in the recovery phase after the return to normal growth conditions (Fig. 7). Taken together, our results can be reconciled by proposing a role for arginine methylation in the regulation of many protein–protein interactions (including but not limited to the TDRD3/DDX3 interaction) important for SG dynamics. This is consistent with, and expands, the model proposed by Denman and colleagues for the recruitment of FMRP to SGs (73). Finally, this interpretation is also reminiscent of the role that arginine methylation plays in other cellular processes; for instance, the assembly of spliceosomal snRNPs, where it serves to promote the efficient and specific assembly of large ribonucleoprotein macromolecular complexes.

### Tudor domains and RNA granules

Several recent studies have provided links between Tudor domain-containing proteins and various types of 'RNA granules'. We have recently uncovered a novel interaction between the Tudor domain of SMN and KSRP, a KH-type RNA-binding protein that colocalizes with SMN in neuronal RNA granules (95). Moreover, each of the novel TDRD3 interactors (including FMRP) have also been identified as components of neuronal RNA granules (51,79,81,96–98). Neuronal granules are considered to be highly related, both in composition and function, to cytoplasmic SGs (98), since

they mediate the transport of specific mRNAs, in a translationally silent state, along dendrites and axons of neuronal cells (99). Whether TDRD3 plays a role in regulating translation within SGs and/or neuronal RNA granules will require further experimentation. In fact, SMN has been shown to relocalize to SGs *per se*, although a functional requirement for its Tudor domain was not established in these studies (67). In our hands, relocalization to SGs was a property unique to the Tudor domain of TDRD3, as the isolated Tudor domains of SMN and SPF30 were not found in SGs under any of the conditions tested here (Fig. 5D and data not shown). Nevertheless, it is possible that the association of SMN with SGs may be cell-type-specific, more transient or may require other domains of the protein (e.g. its C-terminal dimerization domain).

Studies in both *Drosophila* and mouse have uncovered a crucial role for Tudor domain-containing proteins in germline development and polar granules architecture (100–103). Polar or germ granules are specialized structures containing many mRNAs and RNA-binding proteins needed for germ cell formation (104), and it was suggested that several parallels could be drawn between these structures and SGs (98). Sm proteins and PRMT5 were also found to localize to polar granules and to be essential for *Drosophila* germ cell specification and maintenance (105,106). Most importantly, Gonsalvez *et al*. (106) showed that absence of PRMT5 in flies results in the loss of arginine methylation on Sm as well as other proteins, producing a phenotype resembling that of TUDOR mutants, which suggests that methyl-dependent interactions are crucial for this phenomenon. Lastly, DDX3 is thought to play a role in the early phase of spermatogenesis (see below), thus it will be interesting in future studies to look for a role of TDRD3 in germ cell biology.

### TDRD3, SGs and human disease?

TDRD3 can be linked with human genetic diseases. First, DDX3 has a Y-linked homolog (>94% homology) that is also known as DBY. The peptides identified in our proteomic analysis do not allow us to determine if the protein we have isolated was DDX3X or DDX3Y (data not shown). This gene is located in the azospermia factor a (AZFa) region on the human Y chomosome (Yq11.21). Deletion of this Y interval is known to be a major cause for the occurrence of a severe testicular pathology associated with a complete germ cell loss, the SCO syndrome, and specific loss of DBY expression has been documented and correlated with this human pathology (107–109). Secondly, TDRD3 was found to interact with FMRP, the gene associated with fragile X mental retardation syndrome (U. Fischer, personal communication). Thirdly, TDRD3 was identified as one of the top hits in a screen for genes strongly correlated with poor post-operative prognosis of estrogen receptor-negative breast cancers (48). Interestingly, several of the proteins identified in our interaction screen have links with cancer. For example, EWS and FUS are both involved in recurrent chromosome translocations that result in novel fusion oncoproteins associated with many forms of sarcomas (110). These resulting fusion proteins have aberrant transcriptional function compared with their wild-type counterparts and thereby result in a variety of altered cellular properties that contribute to the tumorigenic process. A role for TDRD3 in transcription was never postulated, but a significant proportion (~30%) of total TDRD3 can be detected in the nucleus (Fig. 2). Thus, it would be interesting to investigate the functional relevance of TDRD3 interaction with common sarcoma-associated EWS and FUS oncoprotein fusions. EEF1A1 was found to be overexpressed in rat mammary adenocarcinomas and its expression level correlates with metastasis (111 and references therein). Most strikingly, an oncogenic role for DDX3 was recently shown to be important for breast cancer biogenesis (112). Other components of SGs, including HuR, have also been linked with cancer in many ways (113). Finally, the Tudor domain of TDRD3 is highly conserved with the Tudor domain of SMN, the causative gene of spinal muscular atrophy (17). Whether TDRD3 participates in these pathways, and whether it does so in the context of SGs, remains unclear and will be the focus of future studies.

## MATERIALS AND METHODS

### Cell culture and transfections

The human HeLa cervical carcinoma cell line was purchased from ATCC (Manassas, VA) and grown as a monolayer in DMEM medium supplemented with 1 mM sodium pyruvate, 50 IU/ml penicillin, 50 mg/ml streptomycin and 10% fetal calf serum (Wisent, St-Bruno, QC, Canada). Cells were transfected with DNA plasmids using the Lipofectamine Plus reagent (Invitrogen, Burlington, ON, Canada) according to manufacturer's instructions.

### DNA constructs

Total RNA was extracted from HeLa cells using Trizol reagent (Invitrogen) according to manufacturer's instructions. RNA concentration was measured with a spectrophotometer, and RNA quality was assessed by agarose gel electrophoresis. First strand cDNA synthesis was performed using 5 μg of total RNA and the avian myeloblastosis virus reverse transcriptase (Promega, Madison, WI) with an oligo-dT primer. cDNAs were amplified using oligonucleotides designed to introduce either full-length or deletion mutants of TDRD3 (ΔDUF/OB, ΔN328, ΔUBA, ΔTdr, Δ(DUF/OB+UBA), Δ(DUF/OB+Tdr), DUF/OB, UBA, Central linker and Tdr) in frame with a myc tag into the *Eco*RI and *Xho*I restriction sites of the pCMV-Myc expression vector (Clontech Laboratories Inc., Mountain View, CA). The TDRD3 Tudor (Tdr; amino acids 647–744) fragment was also inserted into the *Eco*RI/*Xho*I sites of the pGEX-4T2 vector (GE Healthcare, Piscataway, NJ). The TDRD3 Tudor E691K mutation was introduced using overlap extension mutagenesis (114) with the following mutagenic oligonucleotides: 5′-ggaaactat**a**aaga ggtgctactg-3′ and 5′-cagtagcacctctt**t**atagtttcc-3′, while using TDRD3-specific primers as flanking oligonucleotides. The mutated fragment was then inserted into the *Eco*RI and *Xho*I restriction sites of both the pCMV-Myc and the pGEX-4T2 vectors. The human SMN Tudor domain was amplified using the following oligonucleotides: 5′-ccggaattcgcagtggaaagttgggg acaaa-3′ and 5′-ccggaattcttaattagctacttcacagattgg-3′, and inserted

into the *Eco*RI restriction site of a modified pcDNA$_{3.1}$ vector (Invitrogen) containing the myc epitope tag sequence (115). Cloning of the wild-type and E134K SMN Tudor domains into the pGEX-4T2 vector have been previously described (17). The Tudor domain of SPF30 was amplified from the SPF30 expression vector (17) by using PCR with the 5′-ttttg aattcttctactcaacctactcattcatgg-3′ and 5′-ttttctcgagttactcctttg ccttccttccttctt-3′ oligonucleotides, and the amplified DNA fragment was inserted into the *Eco*RI and *Xho*I sites of the pcDNA$_{3.1}$-Myc expression vector. Human SERBP1 was amplified from a full-length cDNA clone obtained from Open Biosystems (Huntsville, AL) by using PCR with the 5′-tttttggaattctatgcctgggcacttacaggaagg-3′ and 5′-tttttctcgag attaagccagagctgggaatgcctctgg-3′ oligonucleotides. The amplified DNA fragment was then cloned in frame with a myc tag into the pcDNA$_{3.1}$-Myc expression vector using the same restrictions sites as above. The expression vector encoding the GFP-fused endoribonuclease G3BP protein (59) was a generous gift from Dr Nancy Kedersha (Harvard Medical School, Boston, MA). The pECFP-ER, -Golgi and -Mito vectors were purchased from Clontech. All DNA construct sequences were confirmed by automated DNA sequencing (StemCore Laboratories, Ottawa, ON, Canada).

### Antibodies

A peptide corresponding to the last 22 C-terminal amino acids of TDRD3, $^{723}$DGQPRRSTRPTQQFYQPPRARN$^{744}$, was synthesized at W.M. Keck Foundation Biotechnology Resource Laboratory (Yale University, New Heaven, CT). Polyclonal antibodies were generated by Cedarlane Laboratories (Burlington, ON, Canada) using rabbits injected with the synthetic peptide coupled to KLH. The polyclonal antibodies were affinity-purified over the antigenic peptide coupled to Affi-Gel 10 beads (Bio-Rad, Hercules, CA) following manufacturer's instructions, eluted in 100 mM Glycine pH 2.5, buffered with 1 M Tris–HCl pH 8.0, dialyzed against 1× phosphate-buffered saline (1× PBS: 137 mM NaCl, 2.7 mM KCl, 4.3 mM $Na_2HPO_4$, 1.4 mM $KH_2PO_4$, pH 7.4) at 4°C overnight, and concentrated using Centricon centrifugal devices (Millipore, Bedford, MA). The affinity-purified anti-TDRD3 antibody (0.25 mg/ml) was used at a 1:100 dilution for IF and at a 1:1000 dilution for western blot (IB) analysis.

Monoclonal antibodies against beta-actin (Sigma, St Louis, MO) and glyceraldehyde-3-phosphate dehydrogenase (Covance Canada Inc., Dorval, QC) were both used at a 1:3000 dilution (IB). Goat polyclonal anti-TIA-1 antibody (C-20) and rabbit anti-ribosomal protein L28 (FL-137) antibody were purchased from Santa Cruz Biotechnology (Santa Cruz, CA) and used at 1:50 (IF) and 1:2500 (IB) dilutions, respectively. Mouse anti-FMRP, clone 1C3 (ascites) was purchased from Millipore and used at 1:50 (IF) or 1:2500 (IB) dilutions. Human anti-GW182 (1:600 dilution, IF) and fluorophore-coupled anti-human (1:900 dilution, IF) antibodies were generous gifts from Dr Ken Dimock (University of Ottawa). Rabbit anti-Hsp72 (Hsp72) polyclonal antibody was obtained from Stressgen (Ann Arbor, MI) and used at a 1:10 000 dilution (IB). Rabbit S6 ribosomal protein (5G10) antibody was purchased from Cell Signaling Technology (Danvers, MA) and used at a 1:5000 dilution (IB). The supernatant of a murine hybridoma producing an anti-myc monoclonal antibody (9E10), purchased from ATCC, was used at a 1:50 dilution (IF). Rabbit polyclonal anti-GST antibodies were described elsewhere (17) and used at a 1:5000 dilution (IB). Mouse monoclonal anti-Elongation Factor 1 alpha antibody was purchased from Upstate Biotechnology (Upstate, NY) and used at a 1:3000 dilution (IB). Rabbit polyclonal antibodies directed against the Ewing Sarcoma breakpoint region 1 protein (EWS; 1:40 000 dilution, IB; 1:900 dilution, IF), DEAD box polypeptide 3 (DDX3; 1:1000 dilution, IB; 1:300 dilution, IF), and FUS/TLS (1:40 000 dilution, IB; 1:900 dilution, IF) were all purchased from Bethyl Laboratories Inc. (Montgomery, TX). SYM10 and SYM11 antibodies were described elsewhere (7,9) and were used at a 1:750 and 1:1000 dilution (IB), respectively. Fluorophore-coupled anti-goat, -mouse and -rabbit secondary antibodies were obtained from Jackson ImmunoResearch (West Grove, PA) and used at a 1:100–200 dilution (IF). Horseradish peroxidase-conjugated goat anti-mouse and goat anti-rabbit secondary antibodies (MP Biomedicals, Solon, OH) were used at a 1:4000 dilution.

### Peptide competition assay and Immunoblotting

Fifty microgram of HeLa total protein extracts were resolved on a 10% SDS–PAGE in triplicate, transferred to a PVDF membrane and prepared as three identical western blot strips. PVDF strips were blocked with 5% dry milk in PBST (1× PBS, 0.05% Tween 20) for 1 h at room temperature, and probed with either TDRD3 antibodies (0.25 μg/ml) or an antibody:peptide solution, for 2 h at room temperature. Preadsorbed antibody:peptide solutions were prepared by preincubation of TDRD3 antibodies with a 200-fold molar excess of the antigenic peptide (0.186 μg/ml) or an unrelated synthetic peptide (0.113 μg/ml) in IB solution (1% dry milk in PBST), for 16 h at 4°C. Incubation with primary antibodies was followed by three washes with PBST and probing with secondary antibody under the same conditions. Proteins were detected by chemiluminescence (Millipore) after three final washes in PBST.

### Cell treatments and immunofluorescence

When prepared for indirect IF microscopy, cells were grown directly onto glass cover slips. Transfected HeLa cells were treated 24–48 h post-transfection. Cellular stress response was induced either by treatment with 0.5 mM sodium arsenite for 30 min (oxidative stress; Ars), by incubation at 43°C for 30 min (Heat shock; Hs) or by treatment with 1 M sorbitol for 1 h followed by a 30-min recovery in isotonic culture media (osmotic shock; Osm) (63). To inhibit methylases, HeLa cells were treated for 20 h with 1 mM of the methyltransferase inhibitor MTA (Sigma) prepared in dimethyl sulfoxide (DMSO). Control cells were mock-treated with equal volume of DMSO. Untreated and treated cells were fixed with 4% paraformaldehyde for 10 min, permeabilized with 0.5% Triton X-100 in PBS for 5 min and blocked with 0.1% BSA in PBS for 30 min prior to immunostaining. Cells were incubated with primary antibodies diluted in 0.1% BSA in PBS for 1 h. Cells were then washed once with

0.1% Triton X-100 in PBS, twice with 0.1% BSA in PBS and incubated with the appropriate fluorophore-annexed secondary antibodies in 0.1% BSA in PBS, in the dark, for 1 h. All incubations were performed at room temperature. The cells were washed again as above, counterstained with DAPI and mounted onto glass slides. Fluorescence was visualized with a Z.1 AxioImager upright microscope (Carl Zeiss Canada Ltd, Toronto, ON, Canada) and images were captured with an AXIOCAM HRM R 2.0 CCD digital camera.

### Protein purification

GST-fusion proteins were overexpressed in *Escherichia coli* BL-21 cells (Stratagene, La Jolla, CA) by induction with a final concentration of 0.1 mM isopropyl-D-thiogalactopyranoside (IPTG). Following induction, cells were spun down, resuspended in 10 ml of 1× PBS containing Complete™ protease inhibitor cocktail (Roche Applied Science) and subsequently broken down by sonication (5 pulses of 15 s at 12 watts). Cell debris were discarded through centrifugation for 20 min at 10 000*g*. GST-fusion proteins were then purified using glutathione-agarose (Sigma). For GST pull-down experiments, fusion proteins were kept on glutathione-agarose as a 50% slurry in 1× PBS. Alternatively, GST-fusion proteins were eluted from the beads using 60 mM glutathione in 1× PBS adjusted to pH 7.5. The purified tagged proteins were dialyzed against 1 liter of 1× PBS at 4°C overnight. The dialysates were then concentrated using Amicon centrifugal devices (Millipore). Protein concentration was measured by using the DC protein assay reagent (Bio-Rad).

### Peptide binding assay

Peptide binding assays were performed as previously described (17). Briefly, $(RG)_4$ and $(R^{sDMA}G)_4$ peptides were biotinylated and pre-bound to streptavidin-agarose (Sigma) to generate peptide affinity columns. 0.35–1.4 μg of eluted GST-fusion Tudor domain proteins were diluted in 300 μl of lysis buffer (1% Triton X-100, 20 mM Tris pH 7.4, 150 mM NaCl and Complete™ protease inhibitor cocktail) and mixed with 20 μl of a 50% slurry of the respective peptide affinity column. The mixtures were incubated at 4°C for 30 min with constant end-over-end mixing, and the beads were washed twice with lysis buffer and once with 1× PBS. Retained proteins were then resolved by SDS–PAGE and detected using a rabbit anti-GST serum.

### Pull downs and mass spectrometry

HeLa cells from 5 × 150 mm plates were lysed in lysis buffer for 6 h at 4°C and then centrifuged to remove cellular debris. Cell lysates were incubated with either purified recombinant GST (as a control), GST-TDRD3-Tdr or GST-TDRD3-Tdr E691K proteins coupled to glutathione-agarose for 16 h at 4°C. The beads were then washed twice with lysis buffer and once with 1× PBS. The retained proteins were resolved by SDS–PAGE and the gel, stained with Coomassie Blue. The polypeptides specifically pulled-down by TDRD3-Tdr, that were not pulled-down by GST alone, were excised from the gel and sent out for mass spectrometry analysis and identification (WEMB Biochem Inc., Toronto, ON, Canada). Briefly, gel slices were incubated with trypsin and the resulting digested peptides ran through a matrix-assisted laser desorption ionization-quadrupole-time of flight (MALDI-Qq-TOF) mass spectrometer coupled to a LCQ DECA XP ion trap. The database search for peptide mass fingerprint and MS/MS sequencing data from MALDI-Qq-TOF was done using an in-house database and the Mascot software. Sequencing data generated from the ion trap was analyzed using the Sequest software and a human database subset created from NCBI non-redundant data (68).

### Polysomal profile analysis and protein extraction from sucrose gradient fractions

$5 \times 10^6$ HeLa cells were grown in 100-mm tissue culture dishes, left untreated or incubated with 0.5 mM sodium arsenite for 30 min, harvested and proceeded immediately. Prior to analysis, the cells were resuspended in 1 ml of polysomal buffer [20 mM Tris, pH 7.5, 150 mM NaCl, 1.25 mM $MgCl_2$, 5 U/ml of RNAsine (Amersham Bioscience, Piscataway, NJ), EDTA-free protease inhibitor cocktail (Complete™, Roche) and 1 mM dithiothreitol]. Nonidet P-40 was then added to a final concentration of 1% and cells were lysed for 15 min on ice. Extracts were clarified by centrifugation at 12 000*g* for 20 min at 4°C. Twenty optical density units (260 nm) of cytoplasmic extracts were loaded on each 10–60% linear sucrose gradient and further analyzed as described elsewhere (65). Briefly, following ultracentrifugation (40 000*g* for 4 h) of the sucrose gradients, 0.5-ml fractions were collected using the gradient density fractionator system (Teledyne Isco). mRNPs of each collected fraction were precipitated overnight at −20°C by addition of 1 ml of cold ethanol and centrifuged for 30 min at 14 000*g*. Proteins were then resuspended in 150 ml Laemmli sample buffer.

## FUNDING

I. G. is supported by a scholarship from Fonds de la recherche en santé du Québec. J. C. is the recipient of a Canada Research Chair (Tier 2) in RNA Metabolism and is supported by operating grants # MOP-68943/86746 from CIHR and a grant from Families of Spinal Muscular Atrophy. Funding to pay the Open Access charge was provided by operating grant #MOP-86746 to J.C. from the Canadian Institutes of Health Research.

## ACKNOWLEDGEMENTS

We are grateful to Dr Edouard W. Khandjian and Dr Utz Fischer for their helpful comments in the early phases of this work. We also wish to thank Dr Nancy Kedersha for providing us with useful advice for successful immunofluorescence stainings of stress granules. We would like to thank researchers acknowledged in Material and Methods for providing reagents, as well as Helina Tadesse for critically reading the manuscript. Last but not least, we would like to thank Moaweya Zayed for his help in cloning the Δ(DUF/OB + UBA) and the Δ(DUF/OB + Tdr) constructs.

*Conflicts of Interest statement*. None declared.

## REFERENCES


1. Pawson, T. (2004) Specificity in signal transduction: from phosphotyrosine-SH2 domain interactions to complex cellular systems. *Cell*, **116**, 191–203.
2. Lee, D.Y., Teyssier, C., Strahl, B.D. and Stallcup, M.R. (2005) Role of protein methylation in regulation of transcription. *Endocr. Rev.*, **26**, 147–170.
3. Bedford, M.T. and Richard, S. (2005) Arginine methylation an emerging regulator of protein function. *Mol. Cell*, **18**, 263–272.
4. Cote, J., Boisvert, F.M., Boulanger, M.C., Bedford, M.T. and Richard, S. (2003) Sam68 RNA binding protein is an *in vivo* substrate for protein arginine *N*-methyltransferase 1. *Mol. Biol. Cell*, **14**, 274–287.
5. Boisvert, F.M., Chenard, C.A. and Richard, S. (2005) Protein interfaces in signaling regulated by arginine methylation. *Sci. STKE*, **2005**, re2.
6. Ong, S.E., Mittler, G. and Mann, M. (2004) Identifying and quantifying in vivo methylation sites by heavy methyl SILAC. *Nat. Meth.*, **1**, 119–126.
7. Boisvert, F.M., Cote, J., Boulanger, M.C. and Richard, S. (2003) A proteomic analysis of arginine-methylated protein complexes. *Mol. Cell. Proteomics*, **2**, 1319–1330.
8. Cheng, D., Cote, J., Shaaban, S. and Bedford, M.T. (2007) The arginine methyltransferase CARM1 regulates the coupling of transcription and mRNA processing. *Mol. Cell*, **25**, 71–83.
9. Boisvert, F.M., Cote, J., Boulanger, M.C., Cleroux, P., Bachand, F., Autexier, C. and Richard, S. (2002) Symmetrical dimethylarginine methylation is required for the localization of SMN in Cajal bodies and pre-mRNA splicing. *J. Cell Biol.*, **159**, 957–969.
10. Lukong, K.E. and Richard, S. (2004) Arginine methylation signals mRNA export. *Nat. Struct. Mol. Biol.*, **11**, 914–915.
11. Swiercz, R., Cheng, D., Kim, D. and Bedford, M.T. (2007) Ribosomal protein rpS2 is hypomethylated in PRMT3-deficient mice. *J. Biol. Chem.*, **282**, 16917–16923.
12. Bachand, F. and Silver, P.A. (2004) PRMT3 is a ribosomal protein methyltransferase that affects the cellular levels of ribosomal subunits. *EMBO J.*, **23**, 2641–2650.
13. Bedford, M.T., Frankel, A., Yaffe, M.B., Clarke, S., Leder, P. and Richard, S. (2000) Arginine methylation inhibits the binding of proline-rich ligands to Src homology 3, but not WW, domains. *J. Biol. Chem.*, **275**, 16030–16036.
14. Mowen, K.A., Tang, J., Zhu, W., Schurter, B.T., Shuai, K., Herschman, H.R. and David, M. (2001) Arginine methylation of STAT1 modulates IFNalpha/beta-induced transcription. *Cell*, **104**, 731–741.
15. Kwak, Y.T., Guo, J., Prajapati, S., Park, K.J., Surabhi, R.M., Miller, B., Gehrig, P. and Gaynor, R.B. (2003) Methylation of SPT5 regulates its interaction with RNA polymerase II and transcriptional elongation properties. *Mol. Cell*, **11**, 1055–1066.
16. Kim, J., Daniel, J., Espejo, A., Lake, A., Krishna, M., Xia, L., Zhang, Y. and Bedford, M.T. (2006) Tudor, MBT and chromo domains gauge the degree of lysine methylation. *EMBO Rep.*, **7**, 397–403.
17. Cote, J. and Richard, S. (2005) Tudor domains bind symmetrical dimethylated arginines. *J. Biol. Chem.*, **280**, 28476–28483.
18. Chang, B., Chen, Y., Zhao, Y. and Bruick, R.K. (2007) JMJD6 is a histone arginine demethylase. *Science*, **318**, 444–447.
19. Cuthbert, G.L., Daujat, S., Snowden, A.W., Erdjument-Bromage, H., Hagiwara, T., Yamada, M., Schneider, R., Gregory, P.D., Tempst, P., Bannister, A.J. *et al.* (2004) Histone deimination antagonizes arginine methylation. *Cell*, **118**, 545–553.
20. Wang, Y., Wysocka, J., Sayegh, J., Lee, Y.H., Perlin, J.R., Leonelli, L., Sonbuchner, L.S., McDonald, C.H., Cook, R.G., Dou, Y. *et al.* (2004) Human PAD4 regulates histone arginine methylation levels via demethylimination. *Science*, **306**, 279–283.
21. Callebaut, I. and Mornon, J.P. (1997) The human EBNA-2 coactivator p100: multidomain organization and relationship to the staphylococcal nuclease fold and to the tudor protein involved in *Drosophila melanogaster* development. *Biochem. J.*, **321**, 125–132.
22. Ponting, C.P. (1997) Tudor domains in proteins that interact with RNA. *Trends Biochem. Sci.*, **22**, 51–52.
23. Sprangers, R., Selenko, P., Sattler, M., Sinning, I. and Groves, M.R. (2003) Definition of domain boundaries and crystallization of the SMN Tudor domain. *Acta Crystallogr. Sect. D Biol. Crystallogr.*, **59**, 366–368.
24. Selenko, P., Sprangers, R., Stier, G., Buhler, D., Fischer, U. and Sattler, M. (2001) SMN tudor domain structure and its interaction with the Sm proteins. *Nat. Struct. Biol.*, **8**, 27–31.
25. Maurer-Stroh, S., Dickens, N.J., Hughes-Davies, L., Kouzarides, T., Eisenhaber, F. and Ponting, C.P. (2003) The Tudor domain 'Royal Family': Tudor, plant Agenet, Chromo, PWWP and MBT domains. *Trends Biochem. Sci.*, **28**, 69–74.
26. Barth, S., Liss, M., Voss, M.D., Dobner, T., Fischer, U., Meister, G. and Grasser, F.A. (2003) Epstein-Barr virus nuclear antigen 2 binds via its methylated arginine-glycine repeat to the survival motor neuron protein. *J. Virol.*, **77**, 5008–5013.
27. Brahms, H., Meheus, L., de Brabandere, V., Fischer, U. and Luhrmann, R. (2001) Symmetrical dimethylation of arginine residues in spliceosomal Sm protein B/B' and the Sm-like protein LSm4, and their interaction with the SMN protein. *RNA*, **7**, 1531–1542.
28. Friesen, W.J., Massenet, S., Paushkin, S., Wyce, A. and Dreyfuss, G. (2001) SMN, the product of the spinal muscular atrophy gene, binds preferentially to dimethylarginine-containing protein targets. *Mol. Cell*, **7**, 1111–1117.
29. Hebert, M.D., Shpargel, K.B., Ospina, J.K., Tucker, K.E. and Matera, A.G. (2002) Coilin methylation regulates nuclear body formation. *Dev. Cell*, **3**, 329–337.
30. Charier, G., Couprie, J., Alpha-Bazin, B., Meyer, V., Quemeneur, E., Guerois, R., Callebaut, I., Gilquin, B. and Zinn-Justin, S. (2004) The Tudor tandem of 53BP1: a new structural motif involved in DNA and RG-rich peptide binding. *Structure (Camb.)*, **12**, 1551–1562.
31. Botuyan, M.V., Lee, J., Ward, I.M., Kim, J.E., Thompson, J.R., Chen, J. and Mer, G. (2006) Structural basis for the methylation state-specific recognition of histone H4-K20 by 53BP1 and Crb2 in DNA repair. *Cell*, **127**, 1361–1373.
32. Corsini, L. and Sattler, M. (2007) Tudor hooks up with DNA repair. *Nat. Struct. Mol. Biol.*, **14**, 98–99.
33. Klose, R.J. and Zhang, Y. (2007) Regulation of histone methylation by demethylimination and demethylation. *Nat. Rev. Mol. Cell Biol.*, **8**, 307–318.
34. Ramos, A., Hollingworth, D., Adinolfi, S., Castets, M., Kelly, G., Frenkiel, T.A., Bardoni, B. and Pastore, A. (2006) The structure of the N-terminal domain of the fragile X mental retardation protein: a platform for protein–protein interaction. *Structure*, **14**, 21–31.
35. Roiha, H., Shuster, E.O., Brow, D.A. and Guthrie, C. (1989) Small nuclear RNAs from budding yeasts: phylogenetic comparisons reveal extensive size variation. *Gene*, **82**, 137–144.
36. O'Connell, M.A. and Keegan, L.P. (2006) Drosha versus ADAR: wrangling over pri-miRNA. *Nat. Struct. Mol. Biol.*, **13**, 3–4.
37. Meister, G., Buhler, D., Laggerbauer, B., Zobawa, M., Lottspeich, F. and Fischer, U. (2000) Characterization of a nuclear 20S complex containing the survival of motor neurons (SMN) protein and a specific subset of spliceosomal Sm proteins. *Hum. Mol. Genet.*, **9**, 1977–1986.
38. Friesen, W.J., Paushkin, S., Wyce, A., Massenet, S., Pesiridis, G.S., Van Duyne, G., Rappsilber, J., Mann, M. and Dreyfuss, G. (2001) The methylosome, a 20S complex containing JBP1 and pICln, produces dimethylarginine-modified Sm proteins. *Mol. Cell. Biol.*, **21**, 8289–8300.
39. Pu, W.T., Krapivinsky, G.B., Krapivinsky, L. and Clapham, D.E. (1999) pICln inhibits snRNP biogenesis by binding core spliceosomal proteins. *Mol. Cell. Biol.*, **19**, 4113–4120.
40. Yong, J., Wan, L. and Dreyfuss, G. (2004) Why do cells need an assembly machine for RNA-protein complexes? *Trends Cell Biol.*, **14**, 226–232.
41. Pellizzoni, L. (2007) Chaperoning ribonucleoprotein biogenesis in health and disease. *EMBO Rep.*, **8**, 340–345.
42. Terns, M.P. and Terns, R.M. (2001) Macromolecular complexes: SMN—the master assembler. *Curr. Biol.*, **11**, R862–R864.
43. Pellizzoni, L., Kataoka, N., Charroux, B. and Dreyfuss, G. (1998) A novel function for SMN, the spinal muscular atrophy disease gene product, in pre-mRNA splicing. *Cell*, **95**, 615–624.
44. Meister, G., Hannus, S., Plottner, O., Baars, T., Hartmann, E., Fakan, S., Laggerbauer, B. and Fischer, U. (2001) SMNrp is an essential pre-mRNA splicing factor required for the formation of the mature spliceosome. *EMBO J.*, **20**, 2304–2314.

45. Rappsilber, J., Ajuh, P., Lamond, A.I. and Mann, M. (2001) SPF30 is an essential human splicing factor required for assembly of the U4/U5/U6 tri-small nuclear ribonucleoprotein into the spliceosome. *J. Biol. Chem.*, **276**, 31142–31150.
46. Yang, J., Valineva, T., Hong, J., Bu, T., Yao, Z., Jensen, O.N., Frilander, M.J. and Silvennoinen, O. (2007) Transcriptional co-activator protein p100 interacts with snRNP proteins and facilitates the assembly of the spliceosome. *Nucleic Acids Res.*, **35**, 4485–4494.
47. Shaw, N., Zhao, M., Cheng, C., Xu, H., Saarikettu, J., Li, Y., Da, Y., Yao, Z., Silvennoinen, O., Yang, J. *et al.* (2007) The multifunctional human p100 protein 'hooks' methylated ligands. *Nat. Struct. Mol. Biol.*, **14**, 779–784.
48. Nagahata, T., Onda, M., Emi, M., Nagai, H., Tsumagari, K., Fujimoto, T., Hirano, A., Sato, T., Nishikawa, K., Akiyama, F. *et al.* (2004) Expression profiling to predict postoperative prognosis for estrogen receptor-negative breast cancers by analysis of 25,344 genes on a cDNA microarray. *Cancer Sci.*, **95**, 218–225.
49. Hurley, J.H., Lee, S. and Prag, G. (2006) Ubiquitin-binding domains. *Biochem. J.*, **399**, 361–372.
50. Anderson, P. and Kedersha, N. (2008) Stress granules: the Tao of RNA triage. *Trends Biochem. Sci.*, **33**, 141–150.
51. Kiebler, M.A. and Bassell, G.J. (2006) Neuronal RNA granules: movers and makers. *Neuron*, **51**, 685–690.
52. Kedersha, N., Stoecklin, G., Ayodele, M., Yacono, P., Lykke-Andersen, J., Fritzler, M.J., Scheuner, D., Kaufman, R.J., Golan, D.E. and Anderson, P. (2005) Stress granules and processing bodies are dynamically linked sites of mRNP remodeling. *J. Cell Biol.*, **169**, 871–884.
53. Kedersha, N. and Anderson, P. (2007) Mammalian stress granules and processing bodies. *Methods Enzymol.*, **431**, 61–81.
54. Kozak, M. (1986) Point mutations define a sequence flanking the AUG initiator codon that modulates translation by eukaryotic ribosomes. *Cell*, **44**, 283–292.
55. Yin, J., Sobeck, A., Xu, C., Meetei, A.R., Hoatlin, M., Li, L. and Wang, W. (2005) BLAP75, an essential component of Bloom's syndrome protein complexes that maintain genome integrity. *EMBO J.*, **24**, 1465–1476.
56. Theobald, D.L., Mitton-Fry, R.M. and Wuttke, D.S. (2003) Nucleic acid recognition by OB-fold proteins. *Annu. Rev. Biophys. Biomol. Struct.*, **32**, 115–133.
57. Dolzhanskaya, N., Merz, G. and Denman, R.B. (2006) Oxidative stress reveals heterogeneity of FMRP granules in PC12 cell neurites. *Brain Res.*, **1112**, 56–64.
58. Mazroui, R., Huot, M.E., Tremblay, S., Filion, C., Labelle, Y. and Khandjian, E.W. (2002) Trapping of messenger RNA by fragile X mental retardation protein into cytoplasmic granules induces translation repression. *Hum. Mol. Genet.*, **11**, 3007–3017.
59. Tourriere, H., Chebli, K., Zekri, L., Courselaud, B., Blanchard, J.M., Bertrand, E. and Tazi, J. (2003) The RasGAP-associated endoribonuclease G3BP assembles stress granules. *J. Cell Biol.*, **160**, 823–831.
60. Gilks, N., Kedersha, N., Ayodele, M., Shen, L., Stoecklin, G., Dember, L.M. and Anderson, P. (2004) Stress granule assembly is mediated by prion-like aggregation of TIA-1. *Mol. Biol. Cell*, **15**, 5383–5398.
61. Eystathioy, T., Chan, E.K., Tenenbaum, S.A., Keene, J.D., Griffith, K. and Fritzler, M.J. (2002) A phosphorylated cytoplasmic autoantigen, GW182, associates with a unique population of human mRNAs within novel cytoplasmic speckles. *Mol. Biol. Cell*, **13**, 1338–1351.
62. Eystathioy, T., Jakymiw, A., Chan, E.K., Seraphin, B., Cougot, N. and Fritzler, M.J. (2003) The GW182 protein colocalizes with mRNA degradation associated proteins hDcp1 and hLSm4 in cytoplasmic GW bodies. *RNA*, **9**, 1171–1173.
63. Kedersha, N.L., Gupta, M., Li, W., Miller, I. and Anderson, P. (1999) RNA-binding proteins TIA-1 and TIAR link the phosphorylation of eIF-2 alpha to the assembly of mammalian stress granules. *J. Cell Biol.*, **147**, 1431–1442.
64. Corbin, F., Bouillon, M., Fortin, A., Morin, S., Rousseau, F. and Khandjian, E.W. (1997) The fragile X mental retardation protein is associated with poly(A)+ mRNA in actively translating polyribosomes. *Hum. Mol. Genet.*, **6**, 1465–1472.
65. Khandjian, E.W., Corbin, F., Woerly, S. and Rousseau, F. (1996) The fragile X mental retardation protein is associated with ribosomes. *Nat. Genet.*, **12**, 91–93.
66. Kim, S.H., Dong, W.K., Weiler, I.J. and Greenough, W.T. (2006) Fragile X mental retardation protein shifts between polyribosomes and stress granules after neuronal injury by arsenite stress or in vivo hippocampal electrode insertion. *J. Neurosci.*, **26**, 2413–2418.
67. Hua, Y. and Zhou, J. (2004) Survival motor neuron protein facilitates assembly of stress granules. *FEBS Lett.*, **572**, 69–74.
68. Zhang, R., Barker, L., Pinchev, D., Marshall, J., Rasamoelisolo, M., Smith, C., Kupchak, P., Kireeva, I., Ingratta, L. and Jackowski, G. (2004) Mining biomarkers in human sera using proteomic tools. *Proteomics*, **4**, 244–256.
69. Young, P.J., Francis, J.W., Lince, D., Coon, K., Androphy, E.J. and Lorson, C.L. (2003) The Ewing's sarcoma protein interacts with the Tudor domain of the survival motor neuron protein. *Brain Res. Mol. Brain Res.*, **119**, 37–49.
70. Burt, E.C., Towers, P.R. and Sattelle, D.B. (2006) *Caenorhabditis elegans* in the study of SMN-interacting proteins: a role for SMI-1, an orthologue of human Gemin2 and the identification of novel components of the SMN complex. *Invertebr. Neurosci.*, **6**, 145–159.
71. Saunders, L.R., Perkins, D.J., Balachandran, S., Michaels, R., Ford, R., Mayeda, A. and Barber, G.N. (2001) Characterization of two evolutionarily conserved, alternatively spliced nuclear phosphoproteins, NFAR-1 and -2, that function in mRNA processing and interact with the double-stranded RNA-dependent protein kinase, PKR. *J. Biol. Chem.*, **276**, 32300–32312.
72. Belyanskaya, L.L., Gehrig, P.M. and Gehring, H. (2001) Exposure on cell surface and extensive arginine methylation of ewing sarcoma (EWS) protein. *J. Biol. Chem.*, **276**, 18681–18687.
73. Dolzhanskaya, N., Merz, G., Aletta, J.M. and Denman, R.B. (2006) Methylation regulates the intracellular protein–protein and protein–RNA interactions of FMRP. *J. Cell Sci.*, **119**, 1933–1946.
74. Denman, R.B. (2002) Methylation of the arginine-glycine-rich region in the fragile X mental retardation protein FMRP differentially affects RNA binding. *Cell. Mol. Biol. Lett.*, **7**, 877–883.
75. Kedersha, N., Cho, M.R., Li, W., Yacono, P.W., Chen, S., Gilks, N., Golan, D.E. and Anderson, P. (2000) Dynamic shuttling of TIA-1 accompanies the recruitment of mRNA to mammalian stress granules. *J. Cell Biol.*, **151**, 1257–1268.
76. Liu, G., Grant, W.M., Persky, D., Latham, V.M., Jr, Singer, R.H. and Condeelis, J. (2002) Interactions of elongation factor 1alpha with F-actin and beta-actin mRNA: implications for anchoring mRNA in cell protrusions. *Mol. Biol. Cell*, **13**, 579–592.
77. Yedavalli, V.S., Neuveut, C., Chi, Y.H., Kleiman, L. and Jeang, K.T. (2004) Requirement of DDX3 DEAD box RNA helicase for HIV-1 Rev-RRE export function. *Cell*, **119**, 381–392.
78. Askjaer, P., Rosendahl, R. and Kjems, J. (2000) Nuclear export of the DEAD box An3 protein by CRM1 is coupled to An3 helicase activity. *J. Biol. Chem.*, **275**, 11561–11568.
79. Elvira, G., Wasiak, S., Blandford, V., Tong, X.K., Serrano, A., Fan, X., del Rayo Sanchez-Carbente, M., Servant, F., Bell, A.W., Boismenu, D. *et al.* (2006) Characterization of an RNA granule from developing brain. *Mol. Cell. Proteomics*, **5**, 635–651.
80. Zhou, Z., Licklider, L.J., Gygi, S.P. and Reed, R. (2002) Comprehensive proteomic analysis of the human spliceosome. *Nature*, **419**, 182–185.
81. Kanai, Y., Dohmae, N. and Hirokawa, N. (2004) Kinesin transports RNA: isolation and characterization of an RNA-transporting granule. *Neuron*, **43**, 513–525.
82. Merz, C., Urlaub, H., Will, C.L. and Luhrmann, R. (2007) Protein composition of human mRNPs spliced in vitro and differential requirements for mRNP protein recruitment. *RNA*, **13**, 116–128.
83. Deckert, J., Hartmuth, K., Boehringer, D., Behzadnia, N., Will, C.L., Kastner, B., Stark, H., Urlaub, H. and Luhrmann, R. (2006) Protein composition and electron microscopy structure of affinity-purified human spliceosomal B complexes isolated under physiological conditions. *Mol. Cell. Biol.*, **26**, 5528–5543.
84. You, L.R., Chen, C.M., Yeh, T.S., Tsai, T.Y., Mai, R.T., Lin, C.H. and Lee, Y.H. (1999) Hepatitis C virus core protein interacts with cellular putative RNA helicase. *J. Virol.*, **73**, 2841–2853.
85. Shih, J.W., Tsai, T.Y., Chao, C.H. and Wu Lee, Y.H. (2008) Candidate tumor suppressor DDX3 RNA helicase specifically represses cap-dependent translation by acting as an eIF4E inhibitory protein. *Oncogene*, **27**, 700–714.
86. Heaton, J.H., Dlakic, W.M., Dlakic, M. and Gelehrter, T.D. (2001) Identification and cDNA cloning of a novel RNA-binding protein that

interacts with the cyclic nucleotide-responsive sequence in the Type-1 plasminogen activator inhibitor mRNA. *J. Biol. Chem.*, **276**, 3341–3347.
87. Yang, L., Embree, L.J., Tsai, S. and Hickstein, D.D. (1998) Oncoprotein TLS interacts with serine-arginine proteins involved in RNA splicing. *J. Biol. Chem.*, **273**, 27761–27764.
88. Yang, L., Embree, L.J. and Hickstein, D.D. (2000) TLS-ERG leukemia fusion protein inhibits RNA splicing mediated by serine-arginine proteins. *Mol. Cell. Biol.*, **20**, 3345–3354.
89. Ohkura, N., Yaguchi, H., Tsukada, T. and Yamaguchi, K. (2002) The EWS/NOR1 fusion gene product gains a novel activity affecting pre-mRNA splicing. *J. Biol. Chem.*, **277**, 535–543.
90. Chansky, H.A., Hu, M., Hickstein, D.D. and Yang, L. (2001) Oncogenic TLS/ERG and EWS/Fli-1 fusion proteins inhibit RNA splicing mediated by YB-1 protein. *Cancer Res.*, **61**, 3586–3590.
91. Knoop, L.L. and Baker, S.J. (2001) EWS/FLI alters 5′-splice site selection. *J. Biol. Chem.*, **276**, 22317–22322.
92. Meissner, M., Lopato, S., Gotzmann, J., Sauermann, G. and Barta, A. (2003) Proto-oncoprotein TLS/FUS is associated to the nuclear matrix and complexed with splicing factors PTB, SRm160, and SR proteins. *Exp. Cell Res.*, **283**, 184–195.
93. Yang, L., Chansky, H.A. and Hickstein, D.D. (2000) EWS.Fli-1 fusion protein interacts with hyperphosphorylated RNA polymerase II and interferes with serine-arginine protein-mediated RNA splicing. *J. Biol. Chem.*, **275**, 37612–37618.
94. Neubauer, G., King, A., Rappsilber, J., Calvio, C., Watson, M., Ajuh, P., Sleeman, J., Lamond, A. and Mann, M. (1998) Mass spectrometry and EST-database searching allows characterization of the multi-protein spliceosome complex. *Nat. Genet.*, **20**, 46–50.
95. Tadesse, H., Deschenes-Furry, J., Boisvenue, S. and Cote, J. (2008) KH-type splicing regulatory protein interacts with survival motor neuron protein and is misregulated in spinal muscular atrophy. *Hum. Mol. Genet.*, **17**, 506–524.
96. Villace, P., Marion, R.M. and Ortin, J. (2004) The composition of Staufen-containing RNA granules from human cells indicates their role in the regulated transport and translation of messenger RNAs. *Nucleic Acids Res.*, **32**, 2411–2420.
97. Brendel, C., Rehbein, M., Kreienkamp, H.J., Buck, F., Richter, D. and Kindler, S. (2004) Characterization of Staufen 1 ribonucleoprotein complexes. *Biochem. J.*, **384**, 239–246.
98. Anderson, P. and Kedersha, N. (2006) RNA granules. *J. Cell Biol.*, **172**, 803–808.
99. Sossin, W.S. and DesGroseillers, L. (2006) Intracellular trafficking of RNA in neurons. *Traffic*, **7**, 1581–1589.
100. Arkov, A.L., Wang, J.Y., Ramos, A. and Lehmann, R. (2006) The role of Tudor domains in germline development and polar granule architecture. *Development*, **133**, 4053–4062.
101. Chuma, S., Hosokawa, M., Kitamura, K., Kasai, S., Fujioka, M., Hiyoshi, M., Takamune, K., Noce, T. and Nakatsuji, N. (2006) Tdrd1/Mtr-1, a tudor-related gene, is essential for male germ-cell differentiation and nuage/germinal granule formation in mice. *Proc. Natl. Acad. Sci. USA*, **103**, 15894–15899.
102. Hosokawa, M., Shoji, M., Kitamura, K., Tanaka, T., Noce, T., Chuma, S. and Nakatsuji, N. (2007) Tudor-related proteins TDRD1/MTR-1, TDRD6 and TDRD7/TRAP: domain composition, intracellular localization, and function in male germ cells in mice. *Dev. Biol.*, **301**, 38–52.
103. Smith, J.M., Bowles, J., Wilson, M., Teasdale, R.D. and Koopman, P. (2004) Expression of the tudor-related gene Tdrd5 during development of the male germline in mice. *Geme Expr. Patterns*, **4**, 701–705.
104. Thomson, T. and Lasko, P. (2005) Tudor and its domains: germ cell formation from a Tudor perspective. *Cell Res.*, **15**, 281–291.
105. Anne, J., Ollo, R., Ephrussi, A. and Mechler, B.M. (2007) Arginine methyltransferase Capsuleen is essential for methylation of spliceosomal Sm proteins and germ cell formation in *Drosophila*. *Development*, **134**, 137–146.
106. Gonsalvez, G.B., Rajendra, T.K., Tian, L. and Matera, A.G. (2006) The Sm-protein methyltransferase, dart5, is essential for germ-cell specification and maintenance. *Curr. Biol.*, **16**, 1077–1089.
107. Foresta, C., Ferlin, A. and Moro, E. (2000) Deletion and expression analysis of AZFa genes on the human Y chromosome revealed a major role for DBY in male infertility. *Hum. Mol. Genet.*, **9**, 1161–1169.
108. Kamp, C., Huellen, K., Fernandes, S., Sousa, M., Schlegel, P.N., Mielnik, A., Kleiman, S., Yavetz, H., Krause, W., Kupker, W. *et al.* (2001) High deletion frequency of the complete AZFa sequence in men with Sertoli-cell-only syndrome. *Mol. Hum. Reprod.*, **7**, 987–994.
109. Foresta, C., Ferlin, A., Garolla, A., Moro, E., Pistorello, M., Barbaux, S. and Rossato, M. (1998) High frequency of well-defined Y-chromosome deletions in idiopathic Sertoli cell-only syndrome. *Hum. Reprod.*, **13**, 302–307.
110. Xia, S.J. and Barr, F.G. (2005) Chromosome translocations in sarcomas and the emergence of oncogenic transcription factors. *Eur. J. Cancer*, **41**, 2513–2527.
111. Edmonds, B.T., Wyckoff, J., Yeung, Y.G., Wang, Y., Stanley, E.R., Jones, J., Segall, J. and Condeelis, J. (1996) Elongation factor-1 alpha is an overexpressed actin binding protein in metastatic rat mammary adenocarcinoma. *J. Cell Sci.*, **109**, 2705–2714.
112. Botlagunta, M., Vesuna, F., Mironchik, Y., Raman, A., Lisok, A., Winnard, P., Jr, Mukadam, S., Van Diest, P., Chen, J.H., Farabaugh, P. *et al.* (2008) Oncogenic role of DDX3 in breast cancer biogenesis. *Oncogene*, **27**, 3912–3922.
113. Lopez de Silanes, I., Lal, A. and Gorospe, M. (2005) HuR: post-transcriptional paths to malignancy. *RNA Biol.*, **2**, 11–13.
114. Ho, S.N., Hunt, H.D., Horton, R.M., Pullen, J.K. and Pease, L.R. (1989) Site-directed mutagenesis by overlap extension using the polymerase chain reaction. *Gene*, **77**, 51–59.
115. Chen, T., Damaj, B.B., Herrera, C., Lasko, P. and Richard, S. (1997) Self-association of the single-KH-domain family members Sam68, GRP33, GLD-1 and Qk1: role of the KH domain. *Mol. Cell. Biol.*, **17**, 5707–5718.